ELSEVIER

Precambrian Research 84 (1997) 197–220

Precambrian Research

Neoproterozoic fossils in Mesoproterozoic rocks? Chemostratigraphic resolution of a biostratigraphic conundrum from the North China Platform

Shuhai Xiao [a], Andrew H. Knoll [a,*], Alan J. Kaufman [a], Leiming Yin [b], Yun Zhang [c]

[a] *Botanical Museum, Harvard University, Cambridge, MA 02138, USA*
[b] *Nanjing Institute of Geology and Paleontology, Academia Sinica, Nanjing 210008, China*
[c] *Faculty of Life Sciences, Peking University, Beijing 100871, China*

Received 29 January 1997; accepted 6 June 1997

Abstract

Siliciclastic rocks of the Ruyang Group, southern Shanxi, and the broadly equivalent Gaoshanhe Group, Shaanxi, contain exceptionally well-preserved, large ($\varnothing \approx 150$ μm) acanthomorphic acritarchs recently interpreted as late Neoproterozoic (Sinian, c. 800–544 Ma) in age. This biostratigraphic interpretation is based on the presence of large acanthomorphs in Sinian successions of South China and elsewhere and the perceived absence of comparable forms in older rocks; it casts doubt on the long-accepted interpretation of Ruyang and correlative rocks as Mesoproterozoic in age (1600–1000 Ma). In contrast, thick marine dolomites in overlying units contain abundant radial fibrous fabrics and a narrow range of $\delta^{13}C$ values (c. 0 ± 1‰ vs. PDB), features which characterize unambiguously Mesoproterozoic carbonates elsewhere on the North China Platform and on other continents. Age estimates based on petrofabrics and chemostratigraphy are corroborated by a U–Pb zircon age of 999 Ma (no recorded error) for granites which intrude overlying carbonates. Thus, in combination, the available data constrain the Ruyang siliciclastics and overlying carbonates to be older than about one billion years, making *Shuiyousphaeridium* Yan and other large process-bearing acritarchs from these units among the oldest known distinctly ornamented eukaryotic microfossils. © 1997 Elsevier Science B.V.

Keywords: Acritarchs; Chemostratigraphy; North China Platform; Petrofabrics; Proterozoic

1. Introduction

Few Proterozoic sedimentary successions have been directly and unambiguously dated by radiometric determinations. Therefore, as in Phanerozoic stratigraphy, age estimates for most Proterozoic strata depend on correlation with a small number of radiometrically constrained sections. Stromatolites, microfossils, and, more recently, carbon isotopic profiles have all been used to distinguish between Mesoproterozoic and Neoproterozoic successions, with broad success. Both macrostructures and microfabrics distinguish Mesoproterozoic from Neoproterozoic stromatolites (Komar, 1989; Semikhatov, 1991). Neoproterozoic successions commonly contain large, conspicuously ornamented acritarchs

* Corresponding author. Tel: +1 617 4959306; Fax: +1 617 4959667; e-mail: aknoll@oeb.harvard.edu

PII S0301-9268(97)00029-6

thought to be absent from Mesoproterozoic cherts and shales (Jankauskas, 1989; Knoll and Sergeev, 1995), and at least older Mesoproterozoic carbonate successions studied to date show little of the stratigraphic $\delta^{13}C$ variation documented for Neoproterozoic successions (Knoll et al., 1995). By international agreement, the boundary between the Mesoproterozoic and Neoproterozoic eras has been defined geochronometrically at 1000 Ma (Plumb, 1991). However, the precise relationship of this date to biological, sedimentary and isotopic transitions is unknown.

In this paper, we present an illuminating case history from Proterozoic sedimentary successions on the southwestern margin of the North China Platform (NCP). In these successions, acritarch assemblages of purported Neoproterozoic aspect (Hu and Fu, 1982; Guan et al., 1988; Yan and Zhu, 1992) occur in shales which underlie carbonates containing Mesoproterozoic-style stromatolites (Qiu and Liu, 1982; Liang et al., 1984). New petrological and chemostratigaphic data not only support a Mesoproterozoic age for the successions (and fossils) in question; they tie successions across the NCP to a key section cut by granites radiometrically dated at approximately 1000 Ma. The solution to this regional stratigraphic conundrum has important implications for the broader issues of biostratigraphic correlation and the early diversification of eukaryotic organisms.

2. Regional stratigraphic setting and lithostratigraphy

Proterozoic sedimentary basins are well developed along the margins of the North China Platform (Fig. 1). Regional stratigraphy is best represented by the Jixian Section (Chen et al., 1980; Fig. 2(C)) near Beijing, on the northeastern margin of the NCP, and this serves as the reference section for Chinese stratigraphers. Potentially correlative successions also occur along the northwestern margin of the NCP (Xing, 1989).

On the western and southwestern margins of the NCP, Proterozoic sedimentary rocks generally comprise a siliciclastic-dominated package (i.e. the Gaoshanhe Group and its equivalents), succeeded by a carbonate-dominated package (i.e. the Luonan Group and its equivalents) which is disconformably overlain by tillites of the Luoquan Formation. This succession is well represented in the Zhongtiaoshan and Minor Qinling areas, where Proterozoic sedimentary rocks lie between older metamorphosed or volcanoclastic rocks and Lower Cambrian phosphatic conglomerates. The stratigraphy of two sections sampled for this study, the Shuiyougou Section near Yongji in the northwestern Zhongtiaoshan area, southern Shanxi Province, and the Luonan Section in the Minor Qinling area, Shaanxi Province, is summarized in the following paragraphs.

2.1. The Shuiyougou Section

In the Shuiyougou Section (Figs. 1 and 2(A)), the siliciclastic Ruyang Group rests on Archean crystalline basement (the Sushui Group), for which a metamorphic age of 2350 Ma has been determined (zircon U–Pb, no error reported; quoted in the Bureau of Geology and Mineral Resources of Shanxi Province, 1989). In the northeastern Zhongtiaoshan area, however, Ruyang sediments overlie thick volcanic rocks, mainly andesitic porphyries and volcanoclastics, and interbedded siliciclastic units of the Xiong'er Group. The Xiong'er volcanics, whose geographic distribution mimics the three arms of an ancient triple-junction, accumulated in a Palaeoproterozoic rift basin developed on the southwestern margin of the North China Platform (Sun et al., 1981, 1982).

The Ruyang Group comprises a siliciclastic package which onlapped from south to north over older metamorphic and volcanic rocks. Following the stratigraphic terminology of Guan et al. (1988) in western Henan, the Ruyang Group can be divided (in ascending order) into the Yunmenshan, Baicaoping and Beidajian formations. The Yunmenshan Formation is missing in the section sampled at Shuiyougou. Locally, the Baicaoping Formation consists of purplish or greenish-grey sandstone, with shale increasing upsection. It grades into the overlying Beidajian Formation, which is dominated by siltstones and carbonaceous shales. Acritarchs including *Shuiyousphaeridium*, *Valeria lophostriata*, and *Tappania plana* (Fig. 3) are locally abundant in some horizons in the Beidajian

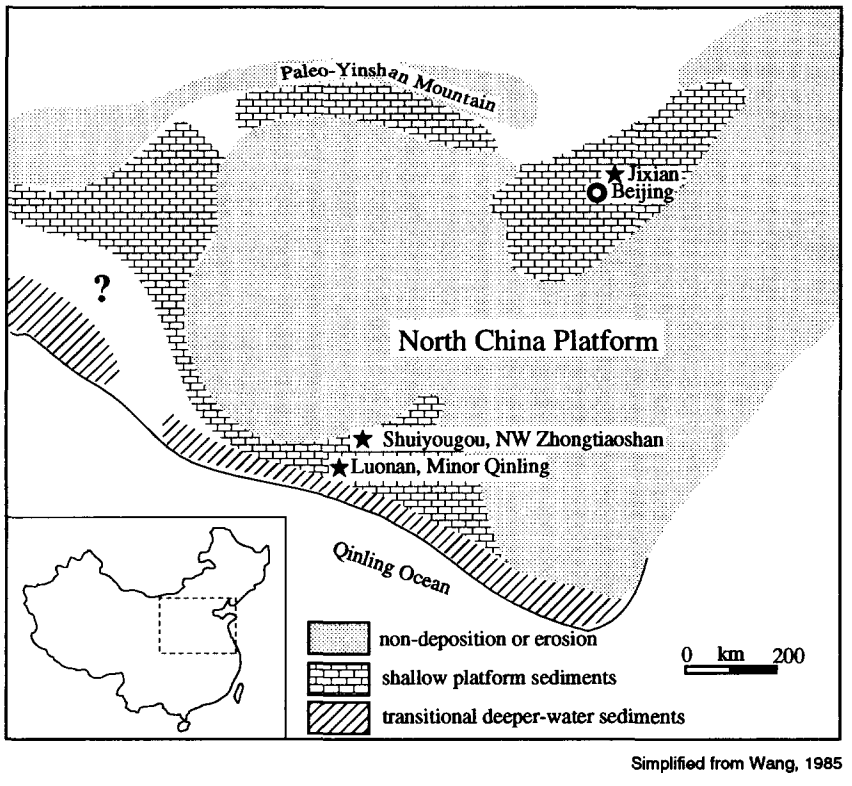

Fig. 1. A simplified Mesoproterozoic paleogeographic map of the North China Platform (modified from Wang, 1985). The Shuiyougou, Luonan and Jixian localities are indicated by stars.

Formation. A 10 m bed of stromatolitic dolorudite marks the top of the Beidajian Formation.

Disconformably overlying the Ruyang Group is the Luoyu Group, which begins with a basal conglomerate about 2 m thick. The lower Luoyu Group consists of the 136-m thick Cuizhuang and Sanjiaotang formations, which cannot be distinguished here as clearly as in the type area in Henan. The siliciclastic portion of these two formations represents a fining-upward half cycle, with the basal conglomerates passing through quartzarenites into a thick succession of greenish-grey shales. The upper half of the Luoyu Group is characterized by peritidal carbonates of the Luoyukou Formation. The 51-m thick Luoyukou Formation begins with a 5-m thick red dolorudite bed, succeeded by red dolomicrosparites and dolomicrites in which fenestral dissolution structures, columnar stromatolites and radial fibrous fabrics (RFFs) are common.

Disconformably overlying the Luoyu Group is the 243-m thick Huanglianduo Formation, a succession of grey, finely laminated dolomites with chert interbeds. A 10-cm thick basal bed of clastic dolomite demarcates its lower boundary with the Luoyukou Formation. Pseudocolumnar stromatolites and dissolution fenestrae are abundant in the lower Huanglianduo Formation, while microdigitate stromatolites and radial fibrous carbonate fabrics (Figs. 4(e–g)) characterize its upper half.

Older rocks are disconformably overlain by the Luoquan Tillite. This unit varies regionally from 0 to >100 m and is only about 10 m thick in the Shuiyougou section. The Luoquan Tillite is interpreted as a continental glacial package, with abundant glaciogenic features such as striated pavements, dropstones and rhythmites (Guan et al., 1986). Its age is controversially thought to be Early Cambrian (Zhu et al., 1994), latest Sinian (Lu et al., 1985; Guan et al., 1986, 1988;

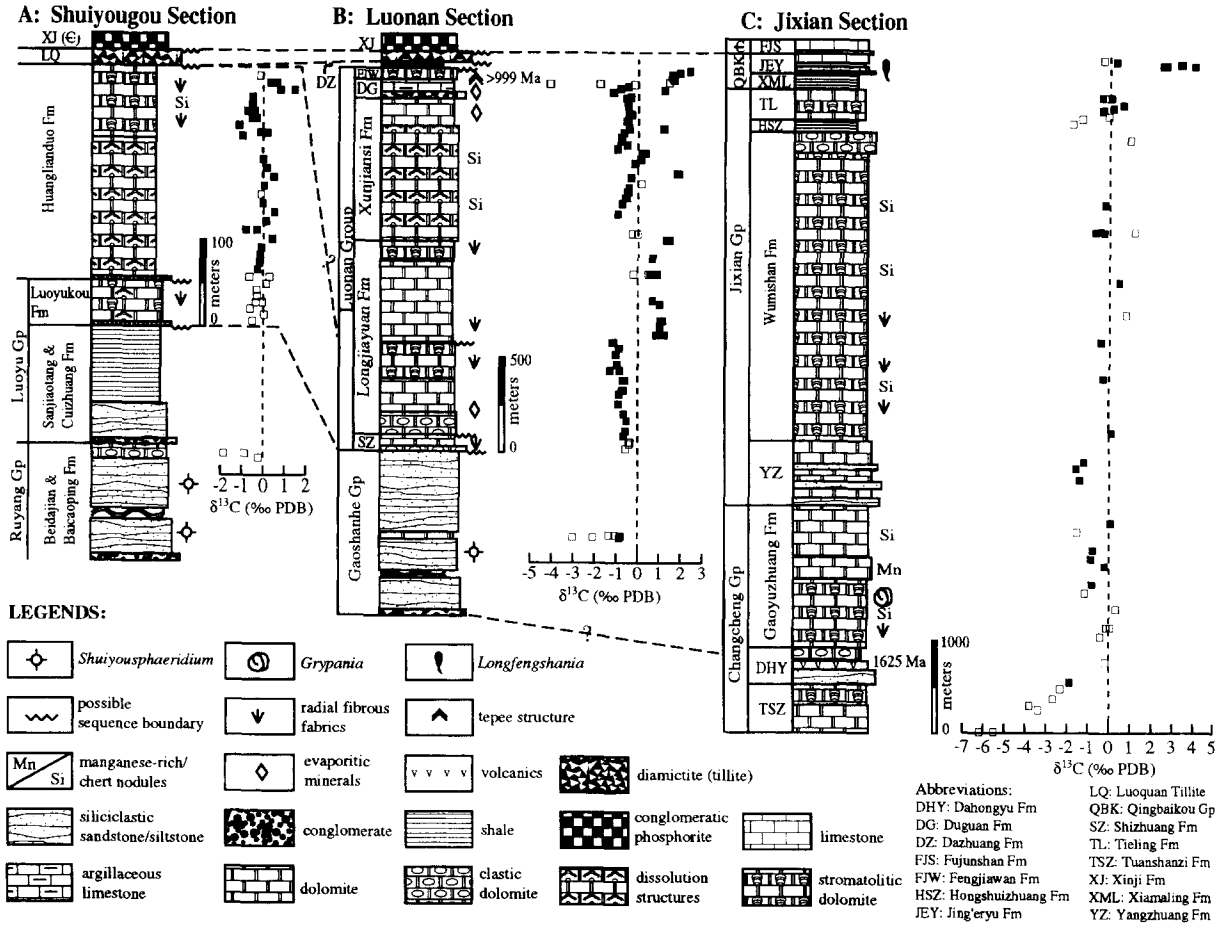

Fig. 2. Stratigraphy and $\delta^{13}C$ plot of the three Proterozoic sections investigated. Solid symbols denote the least altered samples (see text for discussion). (A) the Shuiyougou Section, Yongji, Shanxi; (B) the Luonan Section, Luonan, Shaanxi; (C) the Jixian Section, Jixian, Tianjin. (See Gao et al., 1996 for a sequence stratigraphic interpretation of the Jixian Section.)

Brookfield, 1994) or Varanger/Nantuo (Mu, 1981; Sun et al., 1986). In the Shuiyougou section, phosphatic conglomerates of the Early Cambrian Xinji Formation disconformably overlie the Luoquan Tillite and contain trilobites of the *Bergeroniellus–Huaspis* assemblage, indicating a Botomian age (Zhang and Zhu, 1979; A. Palmer, personal communication).

Fig. 3. (a, b) *Shuiyousphaeridium macroreticulatum* (Du) Yan from the Beidajian Formation, Ruyang Group, the Shuiyougou Section. (a) Microphotograph showing conspicuous processes, reticulate microsculpture and partially preserved veils (arrow). (b) SEM photograph showing details of process morphology. Notice the flaring base and top (arrows). (c) Microphotograph of *Tappania plana* Yin (in press) from the Beidajian Formaition, Ruyang Group, Shuiyougou Section. Notice the neck-like extension to the upper right. (d, e) Microphotographs of *Valeria lophostriata* from the Beidajian Formaition, Ruyang Group, Shuiyougou Section. (e) Close-up of the upper-right part of (d), showing details of concentric striae. (f, g) *Dictyosphaera* vesicles from the Beidajian Formation, Ruyang Group, Shuiyougou Section. Its reticulation is similar to that of *S. macroreticulatum*, but the vesicle is smaller and without processes. (f) Microphotograph. (g) SEM photograph. Scale bar represents 100 μm in (a), 25 μm in (b), 34 μm in (c), 130 μm in (d), 50 μm in (e), 55 μm in (f) and 6 μm in (g).

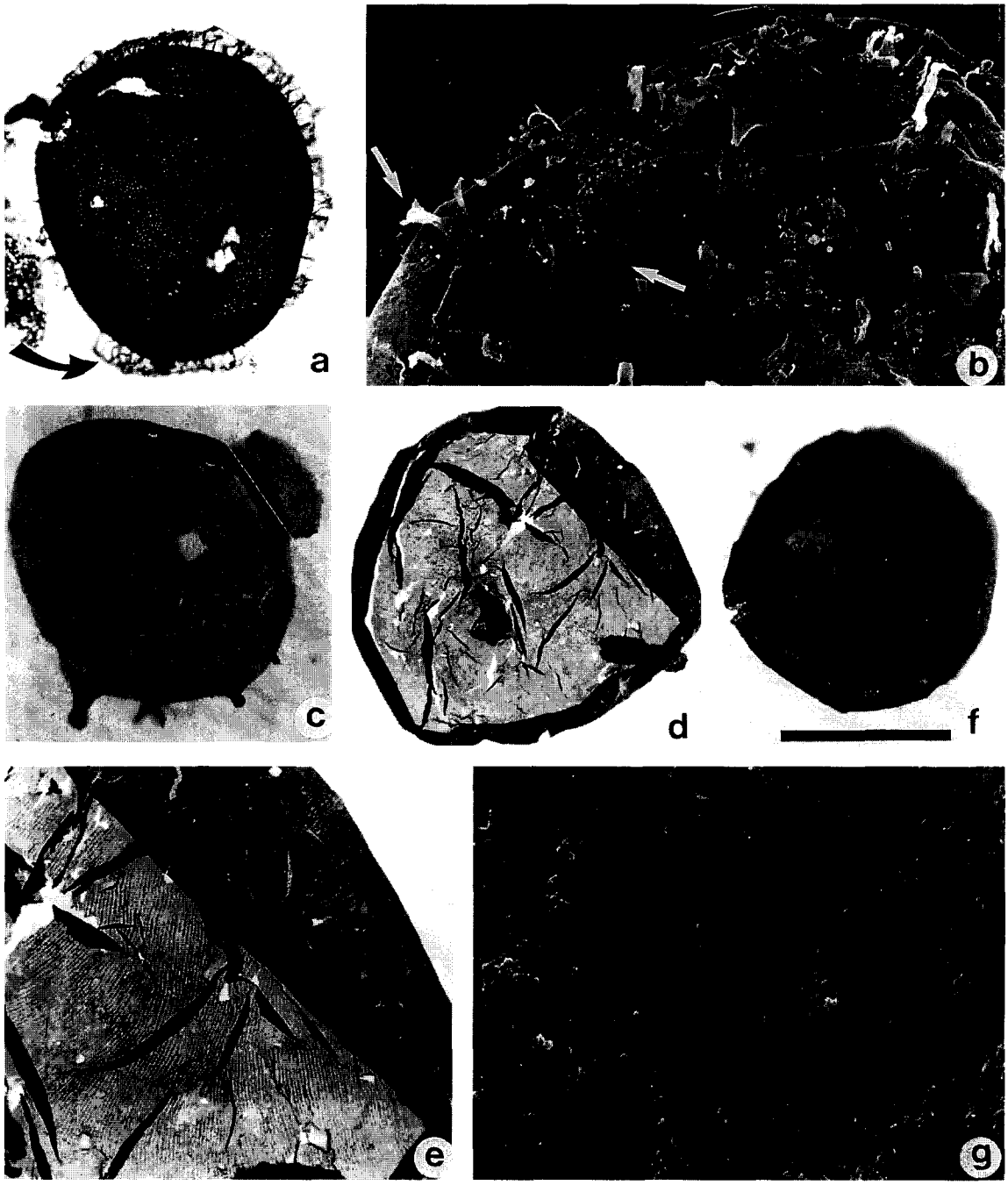

2.2. The Luonan Section

In the Minor Qinling area, about 100 km to the south (basin-ward) of the Shuiyougou Section, Proterozoic successions are similar to those just described but much thicker. The Luonan Section (Figs. 1 and 2(B)), exposed along a trans-Qinling highway from Luonan to Huayin, represents the

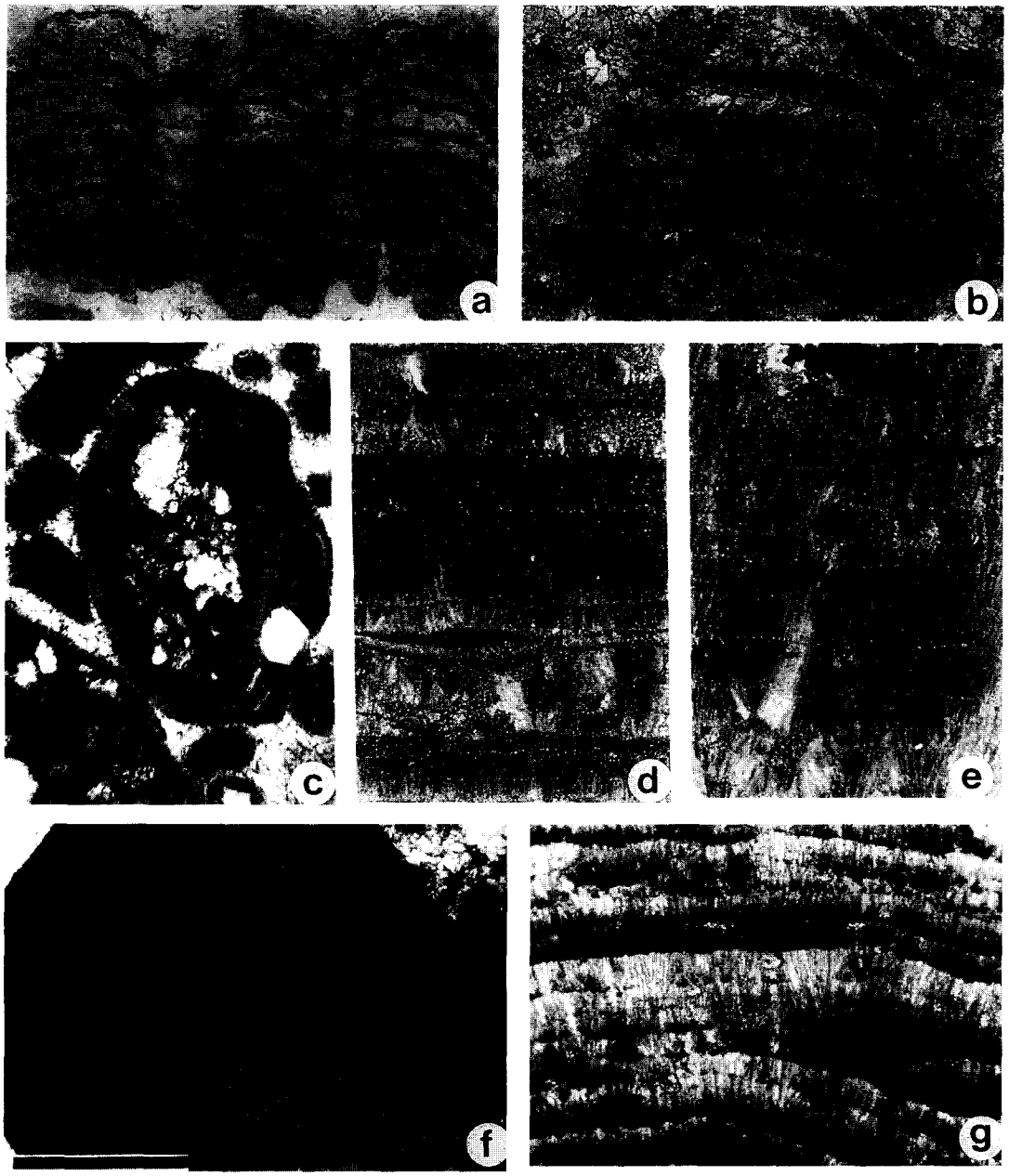

Fig. 4. (a) Microdigitate stromatolite, Longjiayuan Formation (sample #LJY-7.5), Luonan Group, Luonan Section. (b) Close-up (non-polarized light) of the central part of (a), showing mosaic dolomite crystals without any preserved carbonate RFFs (compare with (f)). (c) Dolorudite, uppermost Beidajian Formation (sample #C12), Ruyang Group, Shuiyougou Section, showing isopachous cements encrusting an intraclast (non-polarized light). (d) Carbonate RFFs in microlaminites, Longjiayuan Formation (sample #LJY-14a), Luonan Group, Luonan Section. Precipitates are repeatedly draped by micrite laminae (cross-polarized light). (e) Interpenetration between neighboring fascicles, Huanglianduo Formation (sample #C36a; cross-polarized light). (f) Microdigitate stromatolites from the Huanglianduo Formation (sample #C40) with preserved carbonate RFFs (non-polarized light). (g) Carbonate RFFs in microlaminites of the Huanglianduo Formation (sample #C36a). Notice the contact between the dark and light layers. (h) Square-ended crystal fibers, Longjiayuan Formation (sample #LJY-14a), Luonan Group, Luonan Section (cross-polarized light). (i) Spherulitic cements in *Conophyton* laminae, Longjiayuan Formation (sample #LJY-20), Luonan Group, Luonan Section (cross-polarized light). (j) Gypsum cast, Duguan Formation (sample #DG-6), Luonan Group, Luonan Section (cross-polarized light). (k) Field photograph of teepee structure from the lower Duguan Formation, Luonan Group, Luonan Section. Scale bar represents 2.5 mm in (a), 1 mm in (b), 300 μm in (c), 2 mm in (d) and (e), 3 mm in (f), 900 μm in (g), 190 μm in (h), 1 mm in (i), 330 μm in (j) and 60 mm in (k).

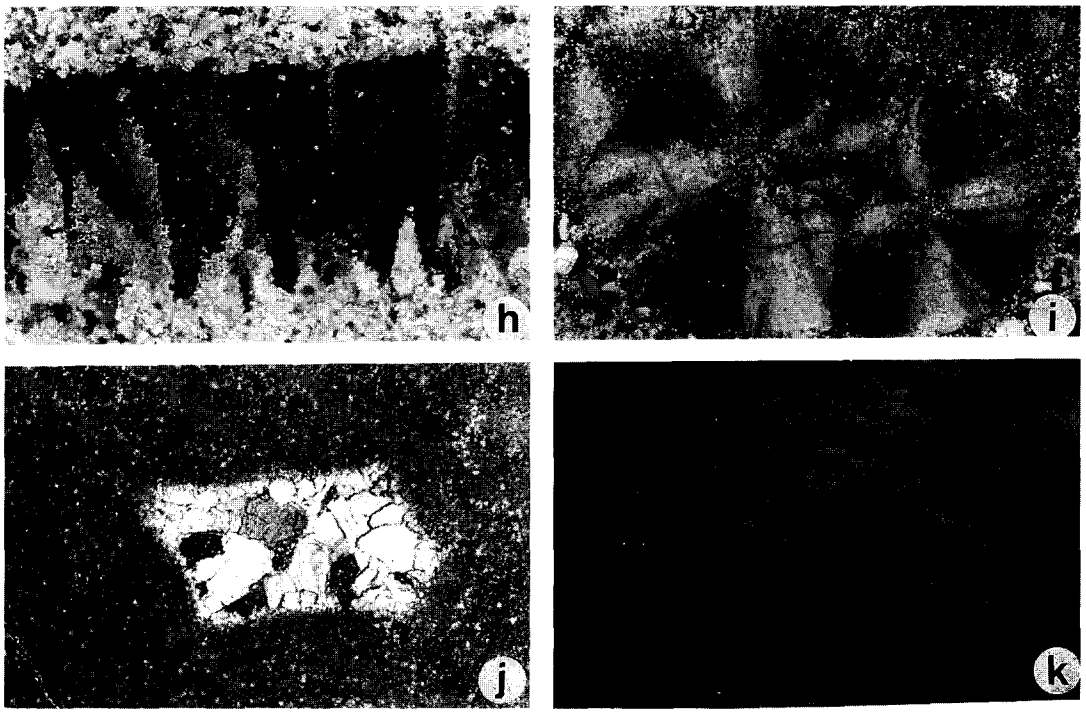

Fig. 4 (*continued*)

typical Proterozoic stratigraphy in the Minor Qinling area.

Resting on Xiong'er volcaniclastic rocks, the c. 4-km thick Gaoshanhe Group consists mostly of slightly metamorphosed quartzarenites and siltstones. It is divided into three formations: in ascending order, the Biegaizi (c. 3000 m, dark-grey organic-rich quartzarenites and siltstones), Erdaohe (c. 700 m, light-grey siltstones with dolomite interbeds) and Chenjiajian (c. 400 m, greenish-grey quartzarenites).

The overlying carbonate package (the Luonan Group) is almost 2000 m thick and can be subdivided (in ascending order) into the Shizhuang, Longjiayuan, Xunjiansi, Duguan and Fengjiawan Formations. Like the Luoyukou Formation in the Shuiyougou Section, the 90-m thick Shizhuang formation begins with a red dolorudite bed (15 m thick), succeeded by red dolomicrosparites. But, unlike the Luoyukou Formation, there is little sign of dissolution in the Shizhuang Formation.

There is an abrupt change from the red dolomites of the Shizhuang Formation to the overlying grey dolomites of the Longjiayuan Formation. Light-grey oomicrosparitic dolomites (with ooids selectively silicified) mark the base of the formation. Above this, the Longjiayuan Formation consists predominantly of grey dolomicrites and dolomicrosparites, with subordinate intramicrosparitic dolomites and late diagenetic chert bands. Gypsum casts have been observed at several horizons in the lower part of this unit. Pseudocolumnar and microdigitate stromatolites with preserved carbonate RFFs (Figs. 4(a, b and d)) are abundant in the middle part. Extremely finely laminated *Omachtenia*-like structures, apparently formed through repeated inundation of seafloor precipitates by thin micritic event beds (Knoll and Semikhatov, in press), are common. A regionally extensive *Conophyton* biostrome occurs near the top of the Longjiayuan Formation; stromatolitic laminae in this biostrome consist entirely of carbonate RFFs. Above the *Conophyton* biostrome, a 2 m chert bed caps the formation.

Above the Longjiayuan Formation, a 5 m siltstone/mudstone interval marks the base of the

Xunjiansi Formation. This 670 m unit is relatively monotonous, consisting predominantly of homogeneous fine to medium crystalline dolomites, with minor dolomicrite and intramicritic dolomite. Seafloor precipitates are less common than in the Longjiayuan Formation. Ripped-up micrite clasts and syneresis structures can be observed in outcrop. Laminated cherts and fenestral dissolution structures are common. Gypsum casts have occasionally been reported.

The lowest meter of the overlying Duguan Formation is a poorly rounded and poorly sorted quartzose diamictite, but the remaining 85 m of this unit is light-grey, purplish-red to buff, thin-bedded dolomicrite and dolomicrosparite with gypsum casts (Fig. 4(j)) preserved at several horizons. Mudcracks, tepee structures (Fig. 4(k)) and brecciated mud clasts are well developed in several horizons throughout the lower and middle part of this unit, suggesting episodic subaerial exposure. The uppermost unit of the Luonan Group is the Fengjiawan Formation, a 45 m succession of light-grey, massive stromatolitic dolomites and grey intramicritic/intramicrosparitic dolomites.

Disconformably overlying the Luonan Group are black, highly carbonaceous and siliceous mudstones of the Dazhuang Formation, which varies from 0 m to over 200 m thick regionally. This unit is missing in the main section along the trans-Qinling highway, but occurs at a satellite section (the Chen'er Section) about 25 km to the east of the main section. The Fengjiawan Formation (or the Dazhuang Formation in the satellite section) is disconformably overlain by the Luoquan Tillite.

2.3. Correlation

The two sections studied are lithologically similar and occur in the same Proterozoic basin, permitting broad lithostratigraphic correlation. The Gaoshanhe Group appears to correlate with the Ruyang Group (and perhaps, the siliciclastic unit in the lower Luoyu Group; Jian et al., 1990), although differing opinions exist (Qiao, 1985; Guan et al., 1988). Direct correlation is supported by the presence of the distinctive *Dictyosphaera–Shuiyousphaeridium* acritarch assemblage in both groups (Hu and Fu, 1982; Yan and Zhu, 1992). The Luoyukou and Huanglianduo formations can be broadly correlated with the Shizhuang and Longjiayuan formations, based on the strikingly similar lithologies and stromatolite assemblages (Qiu and Liu, 1982). New carbonate petrofabric and chemostratigraphic data discussed below support this lithostratigraphic correlation. However, equivalents of the upper Luonan Group and the Shizhuang Formation probably do not exist in the more onshore Shuiyougou Section (see discussion below).

Correlation with the North China reference section at Jixian (Chen et al., 1980; see Fig. 2(C) for the stratigraphic names of the Jixian Section) is less certain. The Ruyang and Gaoshanhe groups have been variously correlated with the Changcheng (Jian et al., 1990), Jixian (Guan et al., 1988), and Qingbaikou groups (Hu and Fu, 1982) in the Jixian region, as well as with Sinian (late Neoproterozoic) successions in South China (Yan and Zhu, 1992; Zhu et al., 1994). Equally, there is no consensus among Chinese stratigraphers on how to correlate the Luoyu and Luonan groups with the Jixian Section.

2.4. Radiometric age constraints

Radiometric dates on the reference section at Jixian are sparse and ambiguous. However, extrusive trachytes in the Dahongyu Formation are dated at 1625 ± 6 Ma (single zircon U–Pb, Lu and Li, 1991). An Ar^{40}/Ar^{39} study on authigenic glauconites in the Tieling Formation yielded ages of 1082 ± 26 and 1171 ± 22 Ma (Li, unpublished data; see Jahn and Cuvellier, 1994). Several glauconite K–Ar ages on Tieling rocks average 1197 ± 18 Ma (range 1134–1236 Ma; Zhong, 1977). On the basis of these dates, it is generally believed that the Jixian Group was deposited during the Mesoproterozoic Era.

Depositional ages of the Proterozoic successions on the southwest margin of the North China Platform are only broadly constrained by radiometric dates on underlying volcanoclastics (the Xiong'er Group) and the biostratigraphy of the overlying Xinji Formation (Botomian, Early Cambrian). Most radiometric dates for the Xiong'er Group and its equivalents fall in the

range 1900–1800 Ma (e.g. a conventional zircon U–Pb age of 1829±17 Ma, a single zircon U–Pb age of 1826±32 Ma, and a SHRIMP U–Pb age of 1840±14 Ma; Sun et al., 1991). However, a few dates from the uppermost volcanics are younger: a 1545 Ma zircon U–Pb age (Li et al., 1985, uncertainty not given) and a 1635±6 Ma whole-rock Rb–Sr age, considered to reflect diagenetic hydrothermal fluid activity (Sun et al., 1991). In western Henan, a granite intruding the Archean basement but truncated by the Ruyang Group has been dated as 1631 Ma (K–Ar on biotite, uncertainty not given; Bureau of Geology and Mineral Resources of Henan Province, 1989). Thus, the lower age limit for both the Ruyang and Gaoshanhe groups appears to be approximately 1600 Ma.

The upper age limit of the Luonan Group is constrained by a single radiometric date. An intrusive biotite granite cutting the Fengjiawan carbonates yields a U–Pb zircon age of 999 Ma (uncertainty not given; The Laboratory of Isotopic Geology, 1974). If the correlation between the Luoyukou plus Huanglianduo and the Shizhuang plus Longjiayuan formations stands, then the Huanglianduo Formation in the Shuiyougou Section cannot be younger than c. 1000 Ma.

In summary, the available radiometric data suggest that, with some uncertainty, the age window of the Ruyang and Luoyu groups, the Huanglianduo Formation, and the Gaoshanhe and Luonan groups approximates the defined boundaries of the Mesoproterozoic Era, i.e. 1600–1000 Ma. This is consistent with most glauconite K–Ar (a handful for the Ruyang Group mostly between 1100 and 1200 Ma; Ma et al., 1980; Guan et al., 1988) and whole-rock Rb–Sr ages (1394±42 Ma from lower Gaoshanhe Group; Li et al., 1985) for these units. This conclusion, however, has been challenged by Yan and Zhu (1992), who argued that large acanthomorphic acritarchs in the Ruyang Group indicate a late Neoproterozoic (Sinian) depositional age.

3. Acanthomorphic acritarchs and biostratigraphy of the Ruyang and Gaoshanhe groups

The most conspicuous element in the Ruyang and Gaoshanhe acritarch assemblage is the large acanthomorphic acritarch taxon first described from the Beidajian Formation in the Shuiyougou Section as *Archaeohystrichosphaeridium macroreticulatum* Du (in Guan et al., 1988). Yan and Zhu (1992) described a similar assemblage from the underlying Baicaoping Formation in the same section, and proposed the new generic name *Shuiyousphaeridium* Yan, because of *Archaeohystrichosphaeridium*'s interpreted status as a junior synonym of *Baltisphaeridium* Eisenack 1958 and *Micrhystridium* Deflandre 1937. Unnamed forms reported earlier from the Gaoshanhe Group (Hu and Fu, 1982) are also fragments of *Shuiyousphaeridium*.

Shuiyousphaeridium macroreticulatum vesicles are c. 150 μm in diameter ($\bar{X}$=148 μm, S_x=38 μm, range=50–300 μm, N=586), with conspicuous branched processes 10–15 μm long and 2–3 μm thick distributed unevenly on the vesicle surface. The processes are open at the distal end and may flare at both base and top (arrows in Fig. 3(b)). The processes appear to be hollow, although this is difficult to determine in compressions. It is unclear whether the processes communicate with the vesicle cavity. A more or less continuous outer membrane (arrow in Fig. 3(a)), supported by processes, may be present. The vesicle surface is covered by fine hexagonal reticulations (Fig. 3(b)), with individual hexagons having maximum dimensions of 1.5–3 μm. The walls of the hexagons are about 0.1–0.3 μm thick and 0.1–0.2 μm high. Fractures corresponding to the reticulations on the outer surface sometimes occur on the inner surface of the vesicles, but this is likely to be a secondary feature. Excystment structures are unknown.

A second acanthomorphic taxon occurs as a rare component of the Beidajian assemblage: *Tappania plana* (Fig. 3(c)) is relatively small (60–70 μm) and has fewer (19–25) but thicker processes and a diagnostic neck-like extension (Yin, 1997).

Dictyosphaera sp. (Figs. 3(f) and (g)) is an abundant component of the Ruyang and Gaoshanhe acritarch assemblage. It has a hexagonal reticulate surface sculpture similar to that of *Shuiyousphaeridium macroreticulatum*, but lacks

processes. The possession of processes might be a developmental phenomenon, as it is the smaller reticulate vesicles which most commonly lack processes. It is also conceivable that some vesicles lost their processes during diagenesis (Knoll, 1984) or sample processing. Therefore, *Dictyosphaera* specimens in the Ruyang and Gaoshanhe groups may be conspecific with *S. macroreticulatum*.

A single specimen of *Valeria lophostriata* (Figs. 3(d) and (e)), with distinctive concentric striations on its vesicle surface, was found in Beidajian macerations. *Leiosphaeridia*, ubiquitously encountered in Proterozoic rocks, is a minor component of this assemblage.

The stratigraphic significance of this acritarch assemblage was discussed by Yan and Zhu (1992), who concluded that the Ruyang Group 'can be correlated with the Sinian (late Neoproterozoic) in South China', because large acanthomorphs are absent in unquestionable Mesoproterozoic successions elsewhere but are characteristic of many late Neoproterozoic successions, including the Doushantuo Formation in South China (Yin and Li, 1978; Yin, 1985, 1987). This interpretation, however, is based on broad grade-level comparisons, and not the distributions of genera or species. *Shuiyousphaeridium* and *Tappania* have never been reported from any unambiguously Neoproterozoic acritarch assemblage, and nor have any unambiguously Neoproterozoic acanthomorph species been identified in the Ruyang Group. To date, the *Shuiyousphaeridium* assemblage is only known from the Gaoshanhe Group in the Minor Qinling area (Hu and Fu, 1982), the Ruyang Group in the Shuiyougou Section (Guan et al., 1988; Yan and Zhu, 1992) and c. 120 km to the east at Mianchi, Henan (L. Yin, unpublished data; C. Yin, personal communication, 1996). Thus, the Ruyang assemblage is a regionally consistent biota of morphologically complex but taxonomically unique acritarchs. Biostratigraphic arguments for a late Neoproterozoic age necessarily rest on weakly supported contentions about grades of evolution.

The long-ranging *Leiosphaeridia* species have little use in correlation. In contrast, widespread occurrences of *Valeria lophostriata* in the Northern Hemisphere are limited to late Mesoproterozoic and early Neoproterozoic strata. This distinctive form has been reported from early Neoproterozoic (Late Riphean) successions of the southern Urals, the Siberian Platform, Scandinavia and North America (see Butterfield and Chandler, 1992; Hofmann and Jackson, 1994), as well as northeast China (Yin, 1987). Recently, it has also been found in the Thule Group of northwestern Greenland and Ellesmere Island, Canada (Dawes and Vidal, 1985; Hofmann and Jackson, 1996; Samuelsson et al., 1997), the Agu Bay Formation of the Fury and Hecla Group, Baffin Island, Arctic Canada (Butterfield and Chandler, 1992), and the Arctic Bay and Society Cliffs formations of the Bylot Supergroup, also on Baffin Island (Hofmann and Jackson, 1994). The three latter occurrences are broadly correlative (Jackson and Iannelli, 1981; Jackson, 1986; Chandler, 1988) and are geochronologically constrained to be younger than Mackenzie dykes (c. 1270 ± 4 Ma; LeCheminant and Heaman, 1989) and older than Franklinian dykes (c. 723 ± 3 Ma; Heaman et al., 1992). Based on paleomagnetic data and U–Pb baddeleyite ages, Knight and Jackson (1994) suggested that the Bylot Supergroup may have been deposited during an 80 Ma interval between 1270 and 1190 Ma. Therefore, the known stratigraphic range of *Valeria lophostriata* is likely to extend back into the Mesoproterozoic.

Clearly, attempts to use acritarchs in constraining depositional ages for the Ruyang and Gaoshanhe groups must rely either on species not known from other formations or taxa whose stratigraphic ranges are long and/or poorly constrained. Independent data are required to evaluate the age of the Ruyang and Gaoshanhe groups and the antiquity of the acanthomorphic acritarchs which they contain.

4. Carbonate fabrics and microdigitate stromatolites

Carbonate radial fibrous fabrics (carbonate RFFs) are abundant in the Luoyukou, Huanglianduo, Shizhuang and Longjiayuan car-

bonates (see Fig. 2 for stratigraphic occurrences), where they occur in microlaminites and in pseudocolumnar, microdigitate and *Conophyton* stromatolites. Under plain light, relatively lighter and thicker fan-bearing laminae (c. 0.1–0.5 mm thick) alternate with darker and thinner (mostly <0.1 mm) dolomicrite or dolomicrosparite (6–50μm) layers (Figs. 4(d) and (g)). The fan fascicles are usually sharply truncated and draped by darker dolomicrosparite laminae. Evidently, carbonate crystals repeatedly nucleated near the sediment–seawater interface, grew upward, and were truncated by exposure or buried by thin event laminae. Within fan-bearing laminae, the individual fascicles, preserved in mosaic dolomite, are usually 0.1–0.5 mm high (about the thickness of a lamina) and 0.5–1.5 mm in maximum width. Some fans, however, penetrate as many as five successive laminae to reach heights of 3 mm. Within the fascicles, individual fibrous crystals (as outlined by organic matter or hematite under plain light, or by optical orientation under cross polarization) are 20–30 μm wide and 400–500 μm long. The excellent preservation of microfabrics in mosaic dolomites of variable crystal size (10–200 μm) suggests that diagenetic stabilization occurred relatively early, so that a near-primary carbon isotopic signature is likely to be preserved (see below). As observed elsewhere (Grotzinger and Read, 1983; Hofmann and Jackson, 1987; Kah, 1997), microdigitate stromatolites in the Luoyukou and Huanglianduo formations and in the lower Luonan Group are essentially stacked, upwardly convex RFF laminae.

RFFs also occur in *Conophyton* biostromes at the top of the Longjiayuan Formation. Upward-diverging precipitate fans similar to those found in laminites are abundant in more or less continuous *Conophyton* laminae. Botryoidal and spherulitic precipitates (Fig. 4(i)) and possible radiaxial fibrous cements are characteristic of more discontinuous, irregular laminae in these stromatolites. Botryoidal and spherulitic bundles have also been reported from subtidal *Conophyton* mounds in the Palaeoproterozoic Rocknest Formation (Grotzinger and Read, 1983).

In dolorudites at the top of the Beidajian Formation, ooids and other intraclasts are commonly coated by isopachous cement 50–150 μm thick (Fig. 4(c)), with individual fibers 5–10 μm across. The isopachous fibers nucleated on intraclast surfaces are shorter and thinner than the RFFs in microlaminites and stromatolites, but are otherwise similar, suggesting that they may have similar origins.

The origin of radial fibrous fabrics in laminated Proterozoic carbonates is controversial. Some authors emphasize a biological genesis by stating that they are remains of calcified red algae (Cao and Zhao, 1978; Liang et al., 1984; Hua and Qiu, 1992). Others suggest that the sheaths of certain microbial mat cyanobacteria such as *Rivularia* may be responsible for the upward-radial fibrous structures (Bertrand-Sarfati, 1976). For the abundant radial fibrous fabrics found in carbonates in Archean through Mesoproterozoic successions, however, the pattern of crystal truncation and interpenetration, and the prismatic cross-sections of crystals imply a chemogenic origin, as pointed out by Grotzinger and Read (1983) and Hofmann and Jackson (1987). These radial fibrous fabrics are morphologically similar to abiogenic aragonite cements, as well as fabrics observed within ooids, vadose pisoliths (Cao and Xue, 1983) and speleothems (Thrailkill, 1976).

RFFs in the Luoyukou, Huanglianduo, Shizhuang and Longjiayuan formations seem unlikely to be remains of red algae or cyanobacteria. Most splays are tightly packed in microlaminae and are sharply truncated by overlying layers (Fig. 4(d), near bottom, and Fig. 4(g)). The radial fibers show no curvature, which would be expected if they were remains of cyanobacterial sheaths or red algae. Instead, RFFs in laminites and stromatolites coexist with and petrographically clearly resemble spherulitic and isopachous cements. Furthermore, square-ended fibers (Fig. 4(h)) and interpenetration between laterally adjacent splays (Fig. 4(e)) are also recognizable. All these observations suggest that these RFFs are the products of essentially abiotic carbonate precipitation, although it is unclear whether the original mineralogy was calcitic or aragonitic. This is not to say that the radial fibrous fabrics have nothing to do with any biological processes.

Although precipitation may have been facilitated by biological processes such as bacterial sulfate reduction (Canfield and Raiswell, 1991), radial fibrous fabrics are not the remains of cyanobacterial sheaths or calcified red algae, and may not be related directly to microbial mats (Grotzinger and Read, 1983; Grotzinger and Knoll, 1995).

Despite the predominantly physicochemical nature of RFFs, they appear to show distinct temporal and spatial trends in Proterozoic carbonate successions, possibly reflecting secular variations in ocean chemistry or atmospheric oxygen levels (Grotzinger and Kasting, 1993; Sumner and Grotzinger, 1996). Whereas micrites, presumably principally formed by whitings, predominate in most Neoproterozoic carbonate successions (Knoll and Swett, 1990), sea-floor cements and precipitates are important constituents of stromatolites and other platform carbonates in Archean and Paleoproterozoic terrains (Grotzinger, 1989, 1993, 1994; Grotzinger and Kasting, 1993; Sami and James, 1996). Of course, micrites also occur in older rocks, and cement may be present in younger rocks: it is the proportional representation that changes. Mesoproterozoic carbonates bridge the two carbonate regimes. Both micrites and sea-floor cements are abundant (Kah and Knoll, 1996), with the latter limited mainly to peritidal facies. Examples include the Jixian Group, especially the Wumishan Formation, in North China (Tianjin Institute of Geology, 1979; Liang et al., 1984; Liang et al., 1985; Cao, 1992), the Kotuikan Formation of the Billyakh Group, northern Siberia (Knoll et al., 1993b), and the Society Cliffs Formation, Baffin Island, Arctic Canada (Kah and Knoll, 1996; Kah, 1997). Like these formations, and in contrast to Neoproterozoic (or, at least, later Neoproterozoic) tidal flats dominated by micrites and microbialites showing evidence of microbial trapping, binding and cementation (e.g. Knoll et al., 1993a), peritidal carbonates of the Luoyukou, Huanglianduo and Longjiayuan formations consist of thick beds dominated by finely laminated sea-floor precipitates.

Microdigitate stromatolites (ministromatolites, asperiform stromatolites, Pseudogymnosolenaceae), with or without radial fabrics depending on preservation, also occur abundantly in Mesoproterozoic and older carbonates (Raaben, 1980; Grey and Thorne, 1985; Grotzinger and Kasting, 1993), but are rare in younger rocks. On the North China Platform, they are conspicuous features of the Mesoproterozoic Jixian Group and its equivalents (Liang et al., 1984). Sea-floor precipitation is the accretional basis of many peritidal stromatolites in Mesoproterozoic carbonates, and is a principal reason why they are so distinctive.

The abundance of sea-floor precipitates (Figs. 4(d, e, g and h)) and microdigitate stromatolites (Figs. 4(a, b and f)) in the Luoyukou, Huanglianduo, Shizhuang and Longjiayuan carbonates therefore suggests that these units and the acanthomorph-yielding siliciclastics which lie beneath them are older than the late Neoproterozoic age inferred by Yan and Zhu (1992). This petrofabric argument is consistent with radiometric dates and age estimates based on stromatolite taxa (Qiu and Liu, 1982; Liang et al., 1984), and is further corroborated by carbon isotopic data.

5. Carbon isotope chemostratigraphy

Carbonates in the Shuiyougou and Luonan sections, along with those of the Proterozoic reference section for North China at Jixian (Chen et al., 1980), were sampled for elemental and isotopic analyses. The analytical procedures used in this study are the same as those described in several previous publications, including Kaufman et al. (1991) and Derry et al. (1992). The results are shown in Table 1, and are plotted against stratigraphic columns in Fig. 2.

5.1. Evaluation of diagenetic alteration

For chemostratigraphy to be meaningful, one must be able to differentiate between true secular variation in the isotopic composition of the surface ocean and diagenetic alteration. For the reasons outlined below, we consider that our $\delta^{13}C$ measurements primarily reflect depositional values rather than a diagenetic overprint.

(1) Microsampling of thick sections was con-

Table 1
Stratigraphic positions, lithologies, and $\delta^{13}C$, $\delta^{18}O$, Mn/Sr, Sr and Mg/Ca analyses of samples reported in this paper

Sample no.[a]	Height (m)[b]	Lithology[c]	$\delta^{13}C$[d]	$\delta^{18}O$[e]	Mn/Sr[f]	Sr (ppm)[f]	Mg/Ca[f]
Beidajian Formation, Ruyang Group, Shuiyougou Section							
C11-(1)	−150.0	Dolointramicrite	—	—	22.7	98.3	—
C11-(2)	−150.0	Dolointramicrite	−0.2	−7.0	11.0	133.1	—
C12	−145.0	Dolointramicrite	−1.8	−10.3	41.2	15.2	—
C12	−145.0	Dolointramicrite	−0.9	−8.8	—	—	—
Luoyukou Formation, Luoyu Group, Shuiyougou Section							
C13	7.0	Dolomicrite	−0.5	−7.3	23.6	28.5	—
C14	14.0	Dolomicrite, S	0.0	−6.5	23.4	12.9	—
C15	21.0	Dolomicrosparite	−0.6	−8.1	37.7	5.1	—
C16-(1)	28.0	Dolomicrosparite	−0.4	−7.5	35.9	16.7	—
C16-(1)	28.0	Dolomicrosparite	0.0	−7.2	—	—	—
C16-(2)	28.0	Dolomicrite, S	−0.4	−7.9	42.2	12.1	—
C17	35.0	Dolomicrite	−0.3	−7.0	32.3	10.3	—
C18	42.0	Dolomicrosparite	−0.3	−7.2	13.8	22.3	—
Huanglianduo Formation, Shuoyougou Section							
C19	49.0	Dolomicrite, S, P	0.1	−5.0	12.3	12.8	—
C20	57.0	Dolomicrosparite	−0.6	−7.6	12.0	30.3	—
C20	57.0	Dolomicrosparite	0.3	−6.0	—	—	—
C21	65.0	Dolomicrite	−0.3	−5.9	7.0	47.9	—
C22	73.0	Dolomicrite	−0.2	−6.6	5.5	11.7	—
C23-(1)	82.0	Dolomicrite	−0.2	−7.1	5.7	14.6	—
C23-(2)	82.0	Dolomicrite	−0.2	−7.0	5.3	23.1	—
C24	90.0	Dolomicrosparite	−0.1	−5.4	6.4	25.9	—
C25	100.0	Dolomicrite	0.4	−6.5	4.5	4.7	—
C26	110.0	Dolomicrite	−0.3	−6.5	6.2	21.6	—
C26	110.0	Dolomicrite	−0.8	−8.1	—	—	—
C27a	120.0	Dolomicrite	0.1	−7.3	2.7	42.5	—
C28	130.0	Dolomicrite	0.5	−5.1	3.2	17.7	—
C29	140.0	Dolomicrite	0.0	−5.3	2.6	88.1	—
C30	150.0	Dolomicrite	−0.1	−6.7	13.1	28.5	—
C31	160.0	Dolomicrite	0.0	−7.2	3.7	11.3	—
C32	170.0	Dolomicrite	0.5	−6.5	6.2	26.6	—
C33	180.0	Dolomicrite	0.2	−8.0	3.1	26.8	—
C33	180.0	Dolomicrite	0.1	−8.5	—	—	—
C34	190.0	Dolomicrite	0.0	−5.6	2.4	31.1	—
C36	216.0	Dolomicrosparite, P	−1.0	−7.2	3.2	17.9	—
C36b	220.0	Dolomicrosparite	−0.1	−5.6	3.0	17.5	—
C36b	220.0	Dolomicrosparite	0.2	−5.1	—	—	—
C37	228.0	Dolomicrite, P	−1.1	−8.5	4.7	14.2	—
C38	236.0	Dolomicrosparite	−0.5	−8.3	3.0	30.8	—
C38	236.0	Dolomicrosparite	−0.3	−8.1	—	—	—
C39	244.0	Dolomicrosparite, P	−0.7	−6.8	2.3	24.1	—
C40	244.0	Dolomicrite, S, P	−0.4	−7.6	4.7	13.9	—
C41	252.0	Dolomicrosparite	−0.5	−6.4	2.7	37.7	—
C42	260.0	Dolomicrite	−0.5	−6.2	4.6	17.9	—
C43	268.0	Dolomicrosparite	0.8	−4.2	3.4	39.6	—
C43	268.0	Dolomicrosparite	1.5	−3.2	—	—	—
C44	276.0	Dolomicrosparite	0.3	−5.7	3.1	7.8	—
C44	276.0	Dolomicrosparite	0.6	−5.5	—	—	—
C45	284.0	Dolomicrosparite, P	−0.1	−7.5	57.0	49.1	—

Table 1 (*continued*)
Stratigraphic positions, lithologies, and $\delta^{13}C$, $\delta^{18}O$, Mn/Sr, Sr and Mg/Ca analyses of samples reported in this paper

Sample no.	Height (m)	Lithology	$\delta^{13}C$	$\delta^{18}O$	Mn/Sr	Sr (ppm)	Mg/Ca
Tuanshanzi Formation, Jixian Section							
TZ 54 (2)	10.0	Dolomicrite	−5.5	−10.0	23.0	92.2	0.3
TZ 54 (1)	10.0	Dolomicrite	−6.2	−11.9	23.9	72.3	0.3
TZ 53	250.0	Dolomicrosparite	−3.4	−8.7	21.1	60.8	0.2
TZ 56	300.0	Dolomicrite	−3.8	−10.4	16.2	96.1	0.3
TZ 57	370.0	Dolomicrite	−2.7	−7.7	15.0	95.1	0.2
TZ 58	480.0	Sandy dolomite	−2.3	−11.2	3.8	72.8	0.0
Dahongyu Formation, Jixian Section							
DG 59	550.0	Sandy dolomite	−1.9	−6.7	4.1	196.7	0.2
DG 60	770.0	Silicified intrasparite	—	—	21.3	34.8	0.3
DG 60-SX	770.0	Intrasparite	−0.2	−8.0	—	—	—
DG 61	900.0	Chert	—	—	14.3	2.6	0.0
Gaoyuzhuang Formation, Jixian Section							
GY 63	1050.0	Dolomicrite	−0.4	−10.3	47.9	25.5	0.3
GY 64 (1)	1150.0	Crystalline dolomite	−0.1	−7.5	45.4	14.3	0.3
GY 64 (2)	1150.0	Crystalline dolomite	0.1	−7.2	89.7	31.5	0.3
GY 64 (2)	1150.0	Crystalline dolomite	−0.1	−9.1	—	—	—
GY 66	1350.0	Dolomicrite	0.3	−6.6	81.5	56.9	0.4
GY 68	1520.0	Dolomicrite	−1.1	−6.5	34.6	33.9	0.3
GY 69	1620.0	Dolomicrosparite	−0.8	−5.5	9.2	—	0.3
GY 71	1820.0	Dolomicrite	−0.2	−6.9	0.4	109.6	0.2
GY 72	1900.0	Dolomicrite	−0.8	−7.3	0.3	258.1	0.1
GY 73	2000.0	Crystalline limestone	−0.8	−6.8	0.0	1696.1	0.0
GY 75	2200.0	Crystalline limestone	−1.5	−11.0	0.1	167.6	0.0
GY 76	2300.0	Crystalline dolomite	0.1	−6.5	1.1	11.5	0.3
Yangzhuang Formation, Jixian Section							
YH 78	2770.0	Dolomicrosparite	−1.4	−9.0	2.4	24.2	0.4
YH 79-SX	2900.0	Limy siltstone	−1.6	−3.6	—	—	
YH 80	2970.0	Dolomicrite	−1.2	−3.3	4.6	27.8	0.4
Wumishan Formation, Jixian Section							
WS 82	3300.0	Dolomicrosparite	0.1	−8.6	2.9	28.0	0.4
WS 84	3900.0	Dolomicrosparite	−0.3	−6.8	2.8	27.1	0.3
WS 86	4105.0	Chert	—	—	8.6	5.5	0.3
WS 87	4300.0	Dolomicrosparite	−0.4	−7.2	2.0	8.2	0.3
WS 88	4400.0	Chert	—	—	19.0	0.7	0.2
WS 89	4600.0	Dolomicrite	0.8	−14.2	0.5	49.7	0.3
WS 91	4950.0	Dolomicrosparite	0.5	−8.2	1.0	27.2	0.3
WS 93	5500.0	Dolomicrosparite	−0.2	−7.0	0.0	12.7	0.6
WS 94	5505.0	Silicified pisolite	1.2	−12.8	—	—	—
WS 94-(1)-SX	5505.0	Silicified pisolite	−0.7	−9.9	—	—	—
WS 95	5510.0	Crystalline dolomite	−0.4	−8.2	0.8	22.6	0.4
WS 96	5800.0	Dolomicrosparite	−0.2	−6.4	0.7	29.1	0.3
WS 97	6500.0	Crystalline dolomite	1.0	−10.5	6.7	15.0	0.4
Tieling Formation, Jixian Section							
TL 98	6680.0	Dolomicrite	−1.8	−6.2	211.5	26.3	0.3
TL 99	6730.0	Dolomicrosparite	−1.3	−5.9	53.8	32.5	0.3
TL 100	6760.0	Dolomicrite	−0.1	−7.9	83.9	37.4	0.3
TL 102	6820.0	Microsparitic limestone	−0.4	−7.6	1.0	95.0	0.0
TL 104-SX	6830.0	Calcite spar, S	−0.3	−7.6	—	—	—
TL 105	6850.0	Calcite spar, S	0.2	−9.7	1.2	65.9	0.0
TL 106	6880.0	Calcite spar, S	0.6	−7.5	3.2	118.9	0.0
TL 108	6960.0	Calcite microspar, S	0.1	−8.6	3.5	110.3	0.0
TL 109	7300.0	Micritic limestone	−0.1	−8.4	10.4	159.5	0.0
TL 109−SX	7300.0	Micritic limestone	−0.4	−8.7	—	—	

Table 1 (*continued*)
Stratigraphic positions, lithologies, and $\delta^{13}C$, $\delta^{18}O$, Mn/Sr, Sr and Mg/Ca analyses of samples reported in this paper

Sample no.	Height (m)	Lithology	$\delta^{13}C$	$\delta^{18}O$	Mn/Sr	Sr (ppm)	Mg/Ca
Jing'eryu Formation, Jixian Section							
JY 109-SX	7305.0	Micritic limestone	4.1	−4.3	—	—	—
JY 110	7310.0	Micritic limestone	2.5	−6.5	2.8	154.7	0.0
JY 110-SX	7310.0	Micritic limestone	2.7	−5.9	—	—	—
JY 111	7325.0	Micritic limestone	3.4	−5.7	2.3	91.5	0.0
JY 111	7325.0	Micritic limestone	—	—	1.1	345.5	0.0
JY 111-SX	7325.0	Micritic limestone	3.5	−5.2	—	—	—
JY 112	7350.0	Micritic limestone	0.3	−9.5	2.7	267.2	0.0
JY 113-SX	7365.0	Micritic limestone	−0.3	−11.1	—	—	—
Fujunshan Formation, Jixian Section							
FS 114-SX	7410.0	Dolomicrosparite	−0.3	−8.6	—	—	—
FS 114-AJK	7410.0	Dolomicrosparite	−1.0	−10.5	—	—	—
Erdaohe Formation, Gaoshanhe Group, Luonan Section							
CEEDH-1	−425.0	Dolomicrosparite	−0.8	−9.1	7.4	64.6	0.5
CEEDH-2	−435.0	Dolomicrite	−0.8	−9.1	5.5	88.5	0.5
EDH-1a	−420.0	Dolomicrosparite	−1.1	−10.9	2.5	177.2	0.5
EDH-1b	−420.0	Dolomicrosparite	−1.3	−12.3	2.2	186.2	0.5
EDH-2-org	−430.0	Dolomicrosparite, ORG	−3.0	−16.6	4.1	264.5	0.4
EDH-2	−430.0	Dolomicrosparite	−2.1	−14.5	2.9	296.7	0.5
Shizhuang Formation, Luonan Group, Luonan Section							
SZ-1	15.0	Dolorudite	−0.6	−8.2	86.3	43.6	0.5
SZ-2a	40.0	Dolomicrosparite	−0.4	−7.9	71.9	22.9	0.5
SZ-2	40.0	Dolomicrosparite	−0.4	−7.6	55.3	28.9	0.5
SZ-3-(1)	50.0	Dolomicrosparite	−0.3	−7.5	81.2	17.9	0.5
SZ-3-(2)	50.0	Dolomicrosparite	−0.4	−8.0	62.8	24.7	0.5
SZ-4	80.0	Dolomicrosparite	−0.7	−9.2	51.3	27.1	0.4
Longjiayuan Formation, Luonan Group, Luonan Section							
LJY-1	105.0	Oomicrosparite	−0.6	−9.0	4.1	41.0	0.6
LJY-2	155.0	Dolomicrosparite	−0.5	−6.0	5.2	25.2	0.5
LJY-3	190.0	Dolomicrite	−0.6	−7.9	6.2	24.4	0.4
LJY-4	240.0	Dolomicrite, E	−0.9	−7.6	3.9	26.4	0.5
LJY-5	290.0	Dolomicrite, E	−0.9	−6.2	3.3	28.5	0.5
LJY-6-(1)	310.0	Dolointramicrudite	−0.7	−7.7	3.8	35.7	0.4
LJY-6-(2)	310.0	Dolointramicrudite	−0.6	−6.5	4.5	25.4	0.5
LJY-7	360.0	Crystalline dolomite	−0.7	−6.0	1.9	30.9	0.4
	360.0	Crystalline dolomite	−0.6	−6.1	2.5	35.8	0.5
LJY-7.5	410.0	Crystalline dolomite, S, P	−0.8	−6.8	4.9	20.2	0.5
LJY-7.5a	410.0	Crystalline dolomite	−1.3	−8.3	4.3	20.9	0.6
LJY-8	440.0	Crystalline dolomite, P	−1.0	−6.1	4.3	22.6	0.5
LJY-9	490.0	Crystalline dolomite, S, P	−1.0	−8.1	3.5	32.6	0.5
LJY-9a	490.0	Crystalline dolomite, S, P	−1.0	−8.0	4.0	26.9	0.6
LJY-10	520.0	Crystalline dolomite, S, P	−0.9	−6.9	1.2	38.1	0.4
LJY-11	550.0	Dolomicrosparite	−1.2	−8.4	1.1	49.7	0.4
LJY-11a-(1)	550.0	Dolomicrosparite	−1.1	−7.2	1.5	35.7	0.4
LJY-11a-(2)	550.0	Dolomicrosparite	−1.2	−7.6	2.2	29.1	0.4
LJY-12-(1)	590.0	Dolomicrosparite	1.1	−8.1	3.7	9.9	0.4
LJY-12-(1)	590.0	Dolomicrosparite	1.2	−9.8	—	—	—
LJY-12-(2)	590.0	Dolomicrosparite	1.2	−7.7	4.4	12.7	0.4
LJY-12a	590.0	Dolomicrosparite	0.8	−8.5	3.8	10.1	0.4
LJY-13	630.0	Dolomicrosparite	1.0	−1.2	3.5	16.4	0.4
LJY-14	660.0	Dolointramicrosparite, P	1.1	−7.8	3.7	16.0	0.4
LJY-14a	660.0	Dolomicrosparite, P	1.2	−8.4	3.1	19.5	0.5
LJY-14a′	660.0	Dolomicrosparite, P	1.1	−8.2	2.6	20.6	0.4

Table 1 (*continued*)

Sample no.	Height (m)	Lithology	$\delta^{13}C$	$\delta^{18}O$	Mn/Sr	Sr (ppm)	Mg/Ca
LJY-15	740.0	Crystalline dolomite	1.0	−7.0	3.6	16.8	0.5
LJY-16	760.0	Crystalline dolomite	0.7	−7.8	1.9	21.8	0.5
LJY-17a	890.0	Crystalline dolomite	0.9	−7.7	2.6	20.6	0.4
LJY-17b-(1)	890.0	Dolomicrosparite	0.5	−10.8	7.4	3.0	0.6
LJY-17b-(2)	890.0	Dolomicrosparite	0.6	−8.8	3.0	16.7	0.5
LJY-17b-(3)	890.0	Dolomicrosparite	−0.2	−12.1	11.9	6.6	0.6
LJY-18	970.0	Dolomicrosparite	0.7	−5.7	1.2	70.4	0.5
LJY-20fan	1060.0	Doloprecipitate, P	1.5	−7.3	11.7	10.1	0.5
LJY-20microspar	1060.0	Dolomicrosparite	1.3	−7.8	5.4	16.4	0.4
Xunjiansi Formation, Luonan Group, Luonan Section							
XJS-1	1091.0	Dolomicrosparite	−0.3	−11.8	—	0.0	0.7(?)
XJS-1a	1091.0	Dolomicrosparite	0.0	−12.2	4.9	7.3	0.6
XJS-2	1190.0	Crystalline dolomite	−0.9	−7.9	1.8	18.3	0.4
XJS-3	1240.0	Dolomicrosparite	−0.7	−6.8	3.1	20.8	0.5
XJS-4	1270.0	Crystalline dolomite	−0.5	−8.1	3.2	20.9	0.5
XJS-4a	1270.0	Crystalline dolomite	−0.6	−7.4	2.3	18.1	0.4
XJS-5	1300.0	Crystalline dolomite	−0.5	−6.0	0.6	62.8	0.4
XJS-5a	1300.0	Crystalline dolomite	−0.4	−8.9	3.0	26.4	0.5
XJS-6	1320.0	Dolomicrosparite	−0.4	−6.6	1.5	53.1	0.5
XJS-7	1340.0	Cherty dolomite	0.2	−13.7	4.3	21.0	0.5
XJS-8	1370.0	Dolomicrosparite	−0.3	−5.7	1.3	60.6	0.5
XJS-9	1390.0	Crystalline dolomite	1.8	−5.8	1.6	49.7	0.4
XJS-9	1390.0	Crystalline dolomite	1.9	−5.9	—	—	—
XJS-10	1440.0	Dolomicrosparite	−0.2	−8.9	1.6	31.0	0.4
XJS-11	1441.0	Crystalline dolomite	−0.1	−9.4	2.2	20.1	0.4
XJS-12	1460.0	Dolomicrite	0.1	−8.6	0.9	43.4	0.4
XJS-13a′	1490.0	Crystalline dolomite	0.3	−9.4	2.2	25.5	0.5
XJS-13	1490.0	Crystalline dolomite	0.4	−15.2	1.8	24.6	0.5
XJS-13a	1490.0	Dolomicrosparite	0.2	−8.1	1.0	52.0	0.5
XJS-14	1510.0	Dolomicrosparite	−1.0	−6.0	0.7	38.2	0.4
XJS-15	1530.0	Crystalline dolomite	−0.5	−7.6	2.4	29.2	0.5
XJS-16	1550.0	Crystalline dolomite	−0.8	−8.2	1.6	25.2	0.4
XJS-16a	1550.0	Crystalline dolomite	−0.8	−8.4	1.6	33.2	0.4
XJS-17	1570.0	Crystalline dolomite	−0.8	−7.1	4.0	14.9	0.4
XJS-18	1590.0	Crystalline dolomite	−0.7	−7.7	3.6	19.6	0.5
XJS-19	1610.0	Crystalline dolomite	−0.4	−7.7	2.4	28.8	0.4
XJS-19a′	1610.0	Crystalline dolomite	1.2	−7.8	5.0	12.8	0.4
XJS-19a′	1610.0	Crystalline dolomite	1.2	−7.7	—	—	—
XJS-20	1630.0	Dolomicrite, E	−0.4	−5.2	0.6	77.9	0.5
XJS-21	1650.0	Dolointramicrite	−0.5	−5.3	1.2	40.1	0.4
XJS-22	1670.0	Dolomicrosparite	−0.5	−8.0	1.7	27.3	0.4
XJS-23	1680.0	Crystalline dolomite	−0.3	−7.2	1.5	32.2	0.5
XJS-24	1700.0	Dolomicrosparite	−0.5	−7.2	2.5	20.9	0.4
XJS-25	1730.0	Dolomicrosparite	−0.5	−6.9	2.7	13.8	0.4
XJS-26	1760.0	Dolomicrosparite	−0.5	−8.8	0.9	100.3	0.5
Duguan Formation, Luonan Group, Luonan Section							
DG-1	1761.0	Diamictite	—	—	—	0.0	0.1
DG-2	1765.0	Crystalline dolomite	−0.3	−7.4	8.3	14.2	0.4
DG-3	1790.0	Dolomicrosparite	−1.1	−3.9	1.9	29.3	0.5
DG-3a	1790.0	Dolomicrosparite	−1.2	−5.2	2.6	40.0	0.5
DG-4	1800.0	Dolomicrite	1.2	−7.5	3.9	14.9	0.5
DG-5	1810.0	Dolomicrite	−0.8	−6.5	3.0	25.6	0.5
DG-6	1820.0	Dolomicrite, E	−0.5	−5.8	2.6	27.2	0.5
DG-7	1830.0	Dolomicrosparite	−0.2	−8.1	65.2	15.7	0.4

Table 1 (*continued*)
Stratigraphic positions, lithologies, and $\delta^{13}C$, $\delta^{18}O$, Mn/Sr, Sr and Mg/Ca analyses of samples reported in this paper

Sample no.	Height (m)	Lithology	$\delta^{13}C$	$\delta^{18}O$	Mn/Sr	Sr (ppm)	Mg/Ca
DG-8	1832.0	Dolomicrite	−1.8	−10.2	20.2	12.1	0.2
DG-8	1832.0	Dolomicrite	−1.8	−9.0	—	—	—
DG-8a	1832.0	Dolomicrite	−4.1	−8.5	24.6	13.7	0.1
DG-8a	1832.0	Dolomicrite	−4.1	−10.0	—	—	—
DG-9	1840.0	Recrystalline dolomite	1.4	−7.2	93.2	11.2	0.5
Fengjiawan Formation, Luonan Section							
FJW-1	1850.0	Dolomicrite, S	1.6	−4.9	3.9	32.5	0.4
FJW-1	1850.0	Dolomicrite, S	1.7	−5.4	—	—	—
FJW-2	1865.0	Dolomicrite	1.6	−5.2	4.1	22.4	0.4
FJW-3-(1)	1875.0	Dolointrasparite	1.6	−5.1	3.3	28.3	0.5
FJW-3-(2)	1875.0	Dolointrasparite	1.6	−6.1	2.6	26.7	0.4
FJW-4	1885.0	Dolointramicrite	1.9	−5.8	2.0	46.4	0.5
FJW-5	1895.0	Dolointramicrite	2.4	−6.2	2.0	47.3	0.5
Luoquan Formation, Luonan Section							
LQ-1	1915.0	Clasts in tillite	—	—	5.2	69.0	0.5
LQ-2	1950.0	Rhythmite	−0.8	−8.0	6.0	62.6	0.4
Dazhuang Formation, Luonan Section							
DZ-1	Carbonaceous mudstone		—	—	1.3	7.6	0.0
DZ-2	Carbonaceous mudstone		—	—	0.7	2.9	0.0
DZ-3	Carbonaceous mudstone		—	—	0.1	54.1	0.0
DZ-4	Carbonaceous mudstone		—	—	7.8	3.5	0.1

[a]Identical sample numbers indicate duplicate runs from the same powder. The suffixes (1), (2), -a, -b, -a′, -SX and -AJK denote subsamples from the same handsample. LJY-20fan is a microsample of precipitates. LJY-20microspar is a microsample of microspars. -org: organic-rich microsample.
[b]For the stratigraphic datum of each section, see Fig. 2.
[c]S: stromatolites, P: precipitates, ORG: organic-rich, E: casts of evaporitic minerals.
[d]The accuracy of the measuring system is better than 0.1‰ PDB for $\delta^{13}C$ (standard runs, $n>20$); —: not determined.
[e]The accuracy of the measuring system is better than 0.3‰ PDB for $\delta^{18}O$ (standard runs, $n>20$). All reported $\delta^{18}O$ values are corrected for dolomite.
[f]—: not determined; 0.0: undetectable.

fined to the least altered portions of samples as indicated by non- to moderate luminescence under cathodoluminescence and petrographic evidence for fabric retention; most samples are from dolomicrites, dolomicrosparites and precipitates.

(2) Crossplots of $\delta^{13}C$–$\delta^{18}O$ show little covariance. A positive correlation between $\delta^{13}C$ and $\delta^{18}O$ has been used to infer $\delta^{13}C$ alteration in samples with low $\delta^{18}O$ (Hudson, 1977; Fairchild et al., 1990). In the Luoyukou and Huanglianduo formations, $\delta^{13}C$ and $\delta^{18}O$ show only moderate covariance (Fig. 5(A); the slope is 0.34 and 0.28, $r^2=0.60$ and 0.47, respectively). However, whereas $\delta^{18}O$ ranges from −3‰ to −9‰ PDB, all but two $\delta^{13}C$ values fall within the narrow range of 0 ± 1‰ PDB. The narrow range of $\delta^{13}C$ values, which contributes to the low slope and high r^2 values of the $\delta^{13}C$–$\delta^{18}O$ regression lines, suggests that the $\delta^{13}C$ values of these formations are stratigraphically consistent, and that any diagenetic alteration of the $\delta^{13}C$ signature is minimal. Crossplots of the Shizhuang, Longjiayuan and Xunjiansi formations (Fig. 5(B)) and of the Mesoproterozoic Gaoyuzhuang, Yangzhuang, Wumishan and Tieling formations in the Jixian Section (Fig. 5(C)) show little covariation between carbon and oxygen isotopes. The $\delta^{13}C$ ranges for those successions are similarly narrow.

(3) Stratigraphic trends are defined by samples with Mn/Sr ≤ 10 and $\delta^{18}O$ values of > -10‰ PDB. Mn/Sr and $\delta^{18}O$ are sensitive indicators of diagenetic alteration in carbonates. Kaufman and Knoll (1995) suggested that carbonates with Mn/Sr less than 10 and $\delta^{18}O$ values greater than

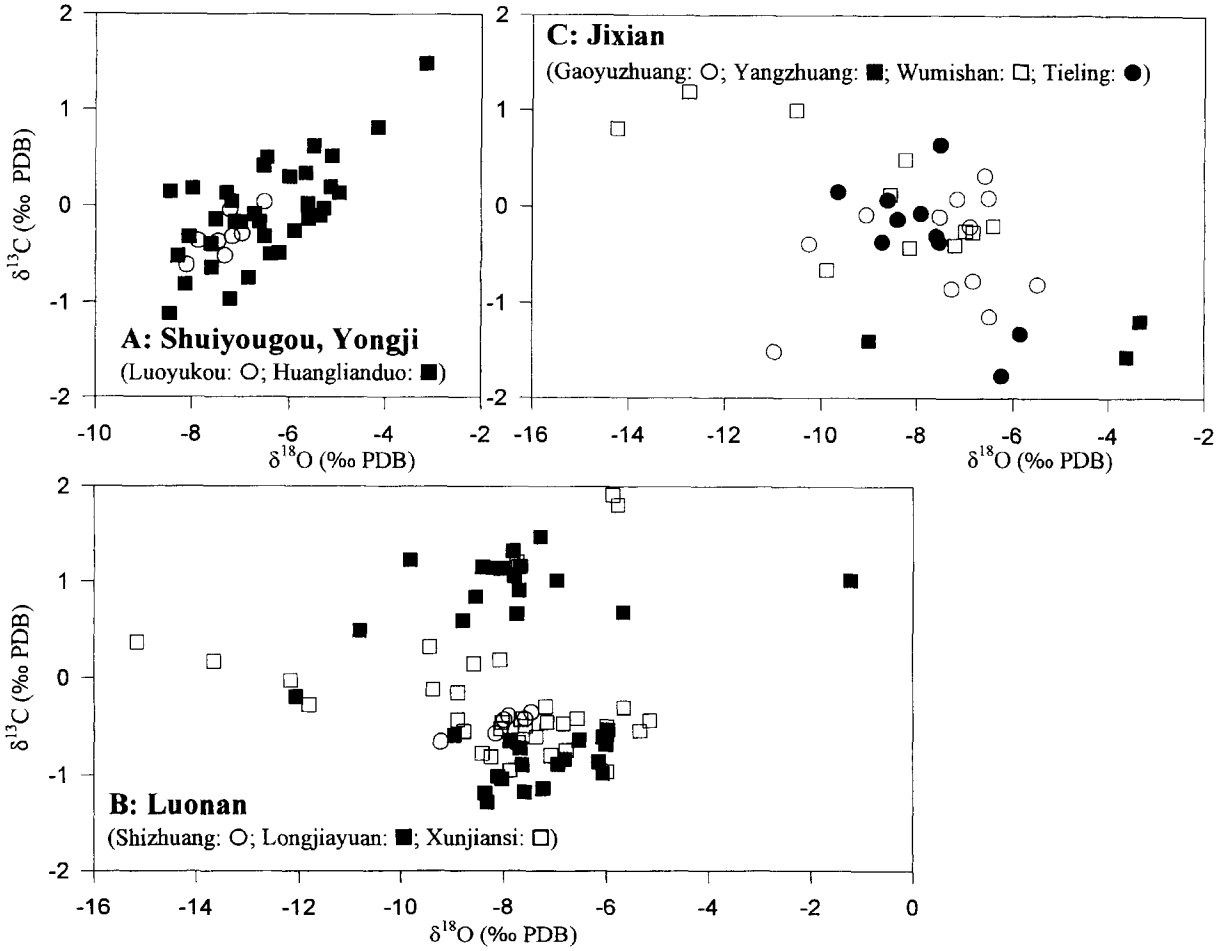

Fig. 5. $\delta^{13}C$–$\delta^{18}O$ cross-plot for the (A) Shuiyougou, (B) Luonan and (C) Jixian sections. Notice the narrow range of $\delta^{13}C$ values within formations.

−10‰ PDB usually retain near-primary $\delta^{13}C$ values. Using these criteria, $\delta^{13}C$ values of samples interpreted as minimally altered are plotted as closed symbols in Fig. 2; samples in which we have less confidence appear as open symbols. It is important to bear in mind that because the carbonate carbon reservoir is large relative to the carbon in diagenetic fluids, $\delta^{13}C$ compositions are less liable to change than are $\delta^{18}O$ and Mn/Sr (Hudson, 1977).

5.2. $\delta^{13}C$ data and interpretation

The most notable characteristic of the $\delta^{13}C$ profiles plotted in Fig. 2 is their lack of stratigraphic variation. The stratigraphic significance of these data is two-fold.

(1) The chemostratigraphic data are consistent with intrabasinal correlations based on lithostratigraphic correlations. Jian et al. (1990) proposed that the Luoyukou plus Huanglianduo formations correlate with the Shizhuang plus Longjiayuan formations, based on similarities in lithostratigraphy and stromatolite assemblages. Both successions have a flat $\delta^{13}C$ profile of 0 ± 1‰ PDB. In the Luonan section, the $\delta^{13}C$ profile shows a sharp 2‰ break between the middle and upper Longjiayuan Formation, suggesting a possible hiatus. Also in the Luonan section, the Duguan

and Fengjiawan formations have slightly different $\delta^{13}C$ signatures than those of underlying carbonates, and show stronger variation. This pattern approximates that seen in latest Mesoproterozoic and earliest Neoproterozoic carbonates in the Turukhansk region, Siberia (Knoll et al., 1995). Similar moderate $\delta^{13}C$ variation also occurs in early Neoproterozoic carbonates of the Jixian Section (Jing'eryu Formation; see Fig. 2(C)), but not in the Shuiyougou Section. Therefore, equivalents of the Duguan, Fengjiawan and Dazhuang formations may not exist in the Shuiyougou Section.

(2) The carbon isotopic profiles exhibited by the Luoyukou, Huanglianduo, Shizhuang, Longjiayuan and Xunjiansi formations closely resemble the stratigraphic pattern of $\delta^{13}C$ variation established for Mesoproterzoic carbonates in the Jixian Section (Fig. 2(C); see also Zhong and Chen, 1992). They also compare closely to profiles which characterize early Mesoproterozoic (>c. 1300 Ma; Kah, 1997) rocks elsewhere, including the Bungle Bungle Dolomite, northwestern Australia (Schidlowski et al., 1983), the Carswell Formation, Canada (Abell et al., 1989), the Gaoyuzhuang and Yangzhuang formations in the Ming Tombs area of North China (Zhou and Zhang, 1991; Zhong and Chen, 1992), the Debengda Formation, northern Siberia (Sergeev et al., 1994), the Billyakh Group, northern Siberia (Knoll et al., 1995), and the Bangemall Group, Australia (Buick et al., 1995). These profiles are markedly different from the pattern of strong $\delta^{13}C$ secular variation established in later Neoproterozoic (c. 850–544 Ma) successions (reviewed by Kaufman and Knoll, 1995). In these younger rocks, $\delta^{13}C$ profiles are characterized by highly positive values (globally up to 10‰ PDB, and locally higher; Iyer et al., 1995) with marked negative excursions to values as low as −4‰ PDB, associated with post-glacial cap carbonates (Kaufman and Knoll, 1995; Kaufman et al., 1997).

Carbonate $\delta^{13}C$ values for the intervening c. 1300–850 Ma interval are few. Existing data from the Mescal Limestone, Arizona (Beeunas and Knauth, 1985), the Hunting Formation, Arctic Canada (Butterfield et al., 1990), Riphean successions in the Turukhansk Uplift, northwestern Siberia (Knoll et al., 1995), and the Society Cliffs Formation, Arctic Canada (Kah, 1997) suggest that during this interval, $\delta^{13}C$ varied more strongly (up to +4‰ PDB) than in the preceding part of the Mesoproterozoic Era, but less strongly than during the later Neoproterozoic. The Fengjiawan and Jin'eryu formations which lie at the top of the Proterozoic successions at Luonan and Jixian, respectively, may belong to this interval (Fig. 2(B) and Fig. 2(C)). The available data thus suggest that carbonates in the Shuiyougou and Luonan sections predate a carbon isotopic transition poorly constrained at 1200–1300 Ma. Certainly, $\delta^{13}C$ chemostratigraphy suggests that sections containing *Shuiyousphaeridium* and associated acritarchs are older than 1000 Ma.

6. Conclusions

The stratigraphic conundrum posed by Proterozoic successions on the southwestern margin of the North China Platform can now be solved. Morphologically complex but taxonomically unique acritarch assemblages of the Ruyang and Gaoshanhe groups do not support a correlation with late Neoproterozoic (Sinian) successions containing diverse acanthomorphic acritarchs. On the contrary, the totality of evidence (radiometric, petrofabric, stromatolitic, litho- and chemostratigraphic) indicates a Mesoproterozoic age for the Ruyang and Luoyu groups, the Huanglianduo Formation, and the Gaoshanhe and Luonan groups.

Acanthomorphic acritarchs are not restricted to Neoproterozoic and younger successions. Consequently, biostratigraphic correlations based on morphological grade rather than taxonomic identity are suspect. In this regard, palynological studies of the Mesoproterozoic/Neoproterozoic transition recall an earlier debate about microfossil asssemblages near the Proterozoic/Cambrian boundary. In the latter case, early evidence that *Skiagia* and other acanthomorphic acritarch genera diversified in the Early Cambrian was interpreted broadly as indicating that acanthomoprhic acritarchs per se are limited to Phanerozoic rocks. The subsequent discovery of large acanthomorphs

in terminal Proterozoic rocks led some researchers to conclude that because the grade-level claim of stratigraphic utility was wrong, all acritarch-based correlations of boundary succession should be viewed as suspect. Of course, the deeper message of the fossils was quite different: terminal Proterozoic and Early Cambrian acritarch assemblages have few if any taxa in common, endowing acritarch biostratigraphy with much explanatory power in boundary correlations (see, for example, Knoll, 1996, and references cited therein).

Our understanding of Mesoproterozoic/Neoproterozoic acritarch assemblages may well follow a similar path. Initial confusion over reports of 'anomalously' old acanthomorphic acritarchs (Hu and Fu, 1982; Yan and Zhu, 1992) may lead to the recognition of distinctive assemblages which will enable us to differentiate between Mesoproterozoic and Neoproterozoic strata and to subdivide Mesoproterozoic successions biostratigraphically. The Ruyang and Gaoshanhe fossils are not the first acanthomorphs to be reported from Mesoproterozoic rocks. More than a decade ago, rare, small acanthomorphs were reported from the late Mesoproterozoic Satka Formation, Ural Mountains (Jankauskas, 1982). A restudy of these materials indicates that purported processes are likely to be diagenetic artefacts. However, unpublished collections made by Jankauskas in Middle Riphean shales from the northern Urals do contain bona fide small (c. 30 μm) acanthomorphic acritarchs (Knoll, personal observation, 1992). The Thule Group in northwest Greenland, once considered to be terminal Proterozoic (Vidal and Dawes, 1980), but now constrained to be late Mesoproterozoic to early Neoproterozoic (Hofmann and Jackson, 1996; Samuelsson et al., 1997; Kah, 1997), also contains large acanthomorphs which appear to be distinct from either the Ruyang fossils or well-characterized Neoproterozoic assemblages (Hofmann and Jackson, 1996; Samuelsson et al., 1997).

The present study also demonstrates that the biostratigraphic and chemostratigraphic transitions which broadly serve to differentiate Mesoproterozoic and Neoproterozoic rocks did not occur instantly or synchronously. While this may defeat simplistic schemes for correlation, it opens up the possibility that, applied in combination, chemo- and biostratigaphy may permit the chronostratigraphic subdivision of Mesoproterozoic time.

Lastly, the observation that acanthomorphic acritarchs began to diversify before 1000 Ma, and probably even before 1200–1300 Ma, corroborates other data (see, for example, Han and Runnegar, 1992; Knoll, 1992; Knoll, 1994; Hofmann, 1994), suggesting that the rapid morphological diversification of eukaryotic organisms inferred from molecular phylogenies (for example Sogin, 1991; Sogin, 1994; Cavalier-Smith et al., 1994) accerelated in the Neoproterozoic Era but began earlier.

Acknowledgments

We thank Professor Jian Wanchou, Qiu Shuyu, Yan Yuzhong and Zhu Shixing for assistance in field work and discussions on local geology. Tadas Jankauskas and the late Gonzalo Vidal made unpublished fossil assemblages available for comparative study. Julie Bartley and Linda Kah provided useful suggestions on early versions of the manuscript. Steve Golubic and Harald Strauss are thanked for their constructive reviews. This study was supported by an NSF grant (DEB-9400712) to A.H.K. and a Graduate Research Grant from the Department of Organismic and Evolutionary Biology at Harvard University to S.X.

References

Abell, P.I., McClory, J., Hendry, H.E., Wheatley, K.L., 1989. Stratigraphic variations in carbon and oxygen isotopes in the dolostone of the Carswell Formation (Proterozoic) of northern Saskatchwan. Can. J. Earth Sci. 26, 2318–2326.

Beeunas, M.A., Knauth, L.P., 1985. Preserved stable isotope signature of subaerial diagenesis in the 1.2 b.y. Mescal Limestone, central Arizona: implications for the timing and development of a terrestrial plant cover. Geol. Soc. Am. Bull. 96, 737–745.

Bertrand-Sarfati, J., 1976. An attempt to classify late Precambrian stromatolite microstructures. In: Walter, M.R. (Ed.), Stromatolites. Elsevier, Amsterdam, pp. 251–259.

Brookfield, M.E., 1994. Problems in applying preservation, facies and sequence models to Sinian (Neoproterozoic) gla-

cial sequences in Australia and Asia. Precambrian Res. 70, 113–143.

Buick, R., DesMarais, D., Knoll, A.H., 1995. Stable isotopic compositions of carbonates from the Mesoproterozoic Bangemall Group, northwestern Australia. Chem. Geol. 123, 153–171.

Bureau of Geology and Mineral Resources of Henan Province, 1989. Regional Geology of Henan Province. Chinese Ministry of Geology and Mineral Resources, Geological Memoirs, Series 1, Number 17. Geological Publishing House, Beijing, 772 pp (in Chinese with English abstract).

Bureau of Geology and Mineral Resources of Shanxi Province, 1989. Regional Geology of Shanxi Province. Chinese Ministry of Geology and Mineral Resources Geological Memoirs, Series 1, Number 18. Geological Publishing House, Beijing, 780 pp (in Chinese with English abstract).

Butterfield, N.J., Chandler, F.W., 1992. Paleoenvironmental distribution of Proterozoic microfossils, with an example from the Agu Bay Formation, Baffin Island. Palaeontology 35, 943–957.

Butterfield, N.J., Knoll, A.H., Swett, K., 1990. A bangiophyte red alga from the Proterozoic of Arctic Canada. Science 250, 104–107.

Canfield, D.E., Raiswell, R., 1991. Carbonate precipitation and dissolution, its relevance to fossil preservation. In: Allison, P.A., Briggs, D.E.G. (Eds.), Taphonomy: Releasing the Data Locked in the Fossil Record. Plenum Press, New York, pp. 411–453.

Cao, R., 1992. A preliminary study on microstructure of the Precambrian stromatolites. In: Qiu, S. Liang, Y. Cao, R., Zhang, L. (Eds.), Late Precambrian Stromatolites and Its Relative Ore Deposits. Northwest University Press, Xi'an, pp. 1–7 (in Chinese with English abstract).

Cao, R., Xue, Y., 1983. Vadose Pisolites of the Tongying Formation (Upper Sinian System) in southwest China. In: Peryt, T.M. (Ed.), Coated Grains. Springer Verlag, Berlin, pp. 538–547.

Cao, R., Zhao, W., 1978. The algal flora of the Tongying (= Dengying) Formation (Upper Sinian System) in southwestern China. Mem. Nanjing Inst. Geol. Palaeontol., Acad. Sinica 10, 1–40.

Cavalier-Smith, T., Alsopp, M.T.E.P., Chao, E.E., 1994. Chimeric conundra: are nucleomorphs and chromists monophyletic or polyphyletic? Proc. Nat. Acad. Sci. USA 91, 11368–11372.

Chandler, F.W., 1988. Geology of the Late Precambrian Fury and Helca Group, Northwest Baffin Island, District of Franklin. Geol. Surv. Canada Bull. 370, 1–30.

Chen, J., Zhang, H., Zhu, S., Zhao, Z., Wang, Z., 1980. Research on Sinian Suberathem of Jixian, Tianjin. In: Tianjin Institute of Geology and Mineral Resources (Ed.), Research in Precambrian Geology, Sinian Suberathem in China. Tianjin Science and Technology Press, Tianjin, pp. 56–114 (in Chinese with English abstract).

Dawes, P.R., Vidal, G., 1985. Proterozoic age of the Thule Group: new evidence from microfossils. Grønl. Geol. Unders. Rep. 125, 22–28.

Derry, L.A., Kaufman, A.J., Jacobsen, S.B., 1992. Sedimentary cycling and environmental change in the Late Proterozoic: evidence from stable and radiogenic isotopes. Geochim. Cosmochim. Acta 56, 1317–1329.

Fairchild, I.J., Marshall, J.D., Bertrand-Sarfati, J., 1990. Stratigraphic shifts in carbon isotopes from Proterozoic stromatolitic carbonates (Mauritania): influences of primary mineralogy and diagenesis. Am. J. Sci. 290A, 46–79.

Gao, L., Zhang, Y., Wang, C., Tian, S., Peng, Y., Liu, Y., Dong, D., He, H., Lei, B., Chen, M., Yang, L., 1996. Meso- and Neoproterozoic sequence stratigraphy in Jixian. Regional Geology of China, No. 1, pp. 64–74 (in Chinese with English abstract).

Grey, K., Thorne, A.M., 1985. Biostratigraphic significance of stromatolites in upward shallowing sequences of the Early Proterozoic Duck Creek Dolomite, Western Australia. Precambrian Res. 29, 183–206.

Grotzinger, J.P., 1989. Facies and evolution of Precambrian carbonate depositional systems: emergence of the modern platform archetype. In: Crevello, P.D., Wilson, J.L., Sarg, J.F., Read, J.F. (Eds.), Controls on Carbonate Platform and Basin Development, SEPM Special Publication No. 44. Tulsa, OK. pp. 79–106.

Grotzinger, J.P., 1993. New views of old carbonate sediments. Geotimes 38 (9), 12–15.

Grotzinger, J.P., 1994. Trends in Precambrian carbonate sediments and their implication for understanding evolution. In: Bengtson, S. (Ed.), Early Life on Earth. Columbia University Press, New York, pp. 245–258.

Grotzinger, J.P., Kasting, J.F., 1993. New constraints on Precambrian ocean composition. J. Geol. 101, 235–243.

Grotzinger, J.P., Knoll, A.H., 1995. Anomalous carbonate precipitates: is the Precambrian the key to the Permian? Palaios 10, 578–596.

Grotzinger, J.P., Read, J.F., 1983. Evidence for primary aragonite precipitation, Lower Proterozoic (1.9 Ga) Rocknest dolomite, Wopmay orogeny, northwest Canada. Geology 11, 710–713.

Guan, B., Geng, W., Rong, Z., Du, H., 1988. The Middle and Upper Proterozoic in the Northern Slope of the Eastern Qinling Ranges, Henan, China. Henan Science and Technology Press, Zhengzhou, 210 pp (in Chinese with English abstract).

Guan, B., Wu, R., Hambrey, M.J., Geng, W., 1986. Glacial sediments and erosional pavements near the Cambrian–Precambrian boundary in western Henan Province, China. J. Geol. Soc. London 143, 311–323.

Han, T.-M., Runnegar, B., 1992. Megascopic eukaryotic algae from the 2.1-billion-year-old Negaunee Iron Formation, Michigan. Science 257, 232–235.

Heaman, L.M., LeCheminant, A.N., Rainbird, R.H., 1992. Nature and timing of Franklin igneous events, Canada: implications for a late Proterozoic mantle plume and the break-up of Laurentia. Earth Planet. Sci. Lett. 109, 117–131.

Hofmann, H.J., 1994. Proterozoic carbonaceous compressions ('metaphytes' and 'worms'. In: Bengtson, S. (Ed.), Early Life

on Earth. Columbia University Press, New York, pp. 342–357.

Hofmann, H.J., Jackson, G.D., 1987. Proterozoic ministromatolites with radial-fibrous fabric. Sedimentology 34, 963–971.

Hofmann, H.J., Jackson, G.D., 1994. Shale-facies microfossils from the Proterozoic Bylot Supergroup, Baffin Island, Canada. Paleontological Society Memoir. Tulsa, OK. 37, 1–35.

Hofmann, H.J., Jackson, G.D., 1996. Notes on the geology and micropaleontology of the Proterozoic Thule Group, Ellesmere Island, Canada and North-West Greenland. Geological Survey of Canada Bulletin No. 495, pp. 1–26.

Hu, Y., Fu, J., 1982. Micropalaeoflora from the Gaoshanhe Formation of Late Precambrian of Luonan, Shaanxi and its stratigraphic significance. Bulletin of the Xi'an Institute of Geology and Mineral Resources, Chinese Academy of Geological Science, No. 4, pp. 102–111 (in Chinese with English abstract).

Hua, H., Qiu, S., 1992. Study on the stromatolites of the Early Jixian System in southern Luonan, Shaanxi Province. In: Qiu, S., Liang, Y., Cao, R., Zhang, L. (Eds.), Late Precambrian Stromatolites and Its Relative Ore Deposits. Northwest University Press, Xi'an, pp. 82–97 (in Chinese with English abstract).

Hudson, J.D., 1977. Stable isotopes and limestone lithification. J. Geol. Soc. London 133, 637–660.

Iyer, S.S., Babinski, M., Krouse, H.R., Chemale, F.J., 1995. Highly ^{13}C-enriched carbonate and organic matter in the Neoproterozoic sediments of the Bambui Group, Brazil. Precambrian Res. 73, 271–282.

Jackson, G.D., 1986. Notes on the Proterozoic Thule Group, northern Baffin Bay. Geological Survey of Canada, Paper 86-1A, pp. 541–552.

Jackson, G.D., Iannelli, T.R., 1981. Rift-related cyclic sedimentation in the Neohelikian Borden Basin, northern Baffin Island. In: Campbell, F.H.A. (ed.), Proterozoic Basins of Canada. Geological Survey of Canada, Paper 81-10, pp. 269–302.

Jahn, B., Cuvellier, H., 1994. Pb–Pb and U–Pb geochronology of carbonate rocks: an assessment. Chem. Geol. 115, 125–151.

Jankauskas, T.V., 1982. Microfossilii Rifeya Yuzhnogo Urala (Riphean microfossils from the Southern Urals). In: Keller, B.M. (Ed.), Stratotyp Rifeya: Paleontologya i Paleomagnetizm (Stratotype of the Riphean: Paleontology and Paleomagnetism). Tr. Geol. Inst. SSSR Akad. Nauk, Moscow, pp. 84–120.

Jankauskas, T.V. (Ed.), 1989. Microfossilii dokembrya SSSR (Precambrian Microfossils of the USSR). Tr. Inst. Geol. Geochronol. Dokembria SSSR Akad. Nauk, Leningrad, 188 pp.

Jian, W., Qiu, S., Liu, H., Yin, F., Wang X., 1990. Subdivision and correlation of the upper Precambrian strata in southwestern border of the North China Platform. In: Jian, W. (Ed.), The Upper Precambrian in the Southwestern Border of the North China Platform. Northwest University Press, Xi'an, pp. 1–12 (in Chinese with English abstract).

Kah, L.C., 1997. Sedimentological, Geochemical and Paleobiological Interactions on a mesoproterozoic carbonate platform: Society cliffs formation, Northern Baffin Island, Arctic Canada. Unpublished PhD Dissertation, Harvard University. 190 pp.

Kah, L.C., Knoll, A.H., 1996. Microbenthic distribution in Proterozoic tidal flats: environmental and taphonomic considerations. Geology 24, 79–82.

Kaufman, A.J., Hayes, J.M., Knoll, A.H., Germs, G.J.B., 1991. Isotopic compositions of carbonates and organic carbon from upper Proterozoic successions in Namibia: stratigraphic variation and the effects of diagenesis and metamorphism. Precambrian Res. 49, 301–327.

Kaufman, A.J., Knoll, A.H., 1995. Neoproterozoic variations in the C-isotope composition of seawater: stratigraphic and biogeochemical implications. Precambrian Res. 73, 27–49.

Kaufman, A.J., Knoll, A.H., Narbonne, G.M., 1997. Isotopes, ice ages, and terminal Proterozoic Earth history. Proc. Nat. Acad. Sci. USA, 94, 6600–6605.

Knight, R.D., Jackson, G.D., 1994. Sedimentology and stratigraphy of the Mesoproterozoic Elwin Subgroup (Aqigilik and Sinasiuvik formations), uppermost Bylot Supergroup, northern Baffin Island. Geol. Surv. Canada Bull. 455, 1–43.

Knoll, A.H., 1984. Microbiotas of the late Precambrian Hunnberg Formation Nordaustlandet, Svalbard. J. Paleontol. 58, 131–162.

Knoll, A.H., 1992. The early evolution of eukaryotes: a geological perspective. Science 256, 622–627.

Knoll, A.H., 1994. Proterozoic and Early Cambrian protists: Evidence for accelerating evolutionary tempo. Proc. Nat. Acad. Sci. USA 91, 6743–6750.

Knoll, A.H., 1996. Archean and Proterozoic paleontology. In: Jansonius, J., McGregor, D.C. (Eds.), Palynology: Principles and Applications, vol. I. AASP Foundation, Tulsa, OK, pp. 51–80.

Knoll, A.H., Fairchild, I.J., Swett, K., 1993. Calcified microbes in Neoproterozoic carbonates: implications for our understanding of the Proterozoic/Cambrian Transition. Palaios 8, 512–525.

Knoll, A.H., Grotzinger, J.P., Sergeev, V.N., 1993. Carbonate precipitation in stratiform and domal structures from the Mesoproterozoic Kotuikan Formation, northern Siberia. Geol. Soc. Am. Abstr. Progr. 25 (6), A357.

Knoll, A.H., Kaufman, A.J., Semikhatov, M.A., 1995. The carbon-isotopic composition of Proterozoic carbonates: Riphean successions from northwestern Siberia (Anabar Massif Turukhansk Uplift). Am. J. Sci. 295, 823–850.

Knoll, A.H., Sergeev, V.N., 1995. Taphonomic and evolutionary changes across the Mesoproterozoic–Neoproterozoic transition. N. Jb. Geol. Palaeont. Abh. 195, 289–302.

Knoll, A.H., Swett, K., 1990. Carbonate deposition during the Late Proterozoic Era: an example from Spitsbergen. Am. J. Sci. 290A, 104–132.

Komar, V.A., 1989. Classification of the microstructures of the Upper Precambrian stromatolites. In: Valdiya, K.S. (ed.), Stromatolites and Stromatolitic Deposits. Himalyan Geology, vol. 13, pp. 229–238.

The Laboratory of Isotopic Geology, Institute of Geology and Mineral Resources, Hupeh, 1974. Isotopic ages of some magmatic and metamorphic rocks from the Yangtze Valley and adjacent regions. Geochimica 1, 32–41 (in Chinese with English abstract).

LeCheminant, A.N., Heaman, L.M., 1989. Mackenzie igneous events, Canada: Middle Proterozoic hotspot magmatism associated with ocean opening. Earth Planet. Sci. Lett. 96, 38–48.

Li, Q., Yang, Y., Jia, J., 1985. The Study of Late Precambrian Strata in the Southern Margin of the North China Platform (Part of Shaanxi Province). Xi'an Jiaotong University Press, Xi'an, 174 pp (in Chinese with English abstract).

Liang, Y., Cao, R., Zhang, L., 1984. Late Precambrian Pseudogymnosolenaceae in China. Geological Publishing House, Beijing, 200 pp (in Chinese with English abstract).

Liang, Y., Zhu, S., Zhang, L., Cao, R., Gao, Z., Bu, D., 1985. Stromatolite assemblage of Late Precambrian in China. Precambrian Res. 29, 15–32.

Lu, S., Li, H., 1991. A precise U–Pb single zircon age determination for the volcanics of the Dahongyu Formation, Changcheng System in Jixian. Bull. Chinese Acad. Geol. Sci. 22, 137–146.

Lu, S., Ma, G., Gao, Z., Lin, W., 1985. Sinian ice ages and glacial sedimentary facies-areas in China. Precambrian Res. 29, 53–63.

Ma, G., Liu, S., Deng, Z., 1980. The K–Ar dating of the glauconite from the Ruyang Group of the Upper Precambrian, western Henan and its stratigraphic correlation. Bull. Yichang Inst. Bull. Yichang Inst. Geol. Mineral Resources, Chinese Acad. Geol. Sci. 1, 103–112.

Mu, Y., 1981. Luoquan tillite of the Sinian System in China. In: Hambrey M.J., Harland W.B. (Eds.), Pre-Pleistocene Glacial Record, IGCP 38. Cambridge University Press, Cambridge, pp. 402–413.

Plumb, K., 1991. New Precambrian time scale. Episodes 14, 139–140.

Raaben, M.E., 1980. Microstromatolites as a characteristic element of the Lower Proterozoic stromatolitic assemblages. Dokl. Akad. Nauk SSSR 250 (3), 734–737.

Qiao, X., 1985. Columnar Sections of the Middle and Upper Proterozoic (1850–850 m.y. BP) in North China. In: Wang, H. (Ed.), Atlas of the Palaeogeography of China. Cartographic Publishing House, Beijing, p. 7 (in Chinese with English abstract).

Qiu, S., Liu, H., 1982. Stromatolitic assemblages and their stratigraphic significance from the Upper Precambrian rocks in the Minor Qinling Range in Shaanxi Province. J. Northwest Univ. (Special Issue on Precambrian) 1982, 1–33.

Sami, T.T., James, N.P., 1996. Synsedimentary cements as paleoproterozoic platform building blocks Pethei Group, northwestern Canada. J. Sed. Res. 66, 209–222.

Samuelsson, S., Dawes, P.R., Vidal, G., 1997. Acid-resistant palynomorphs from the Proterozoic Thule Supergroup, North-West Greenland. Palaeontol., in press.

Schidlowski, M., Hayes, J.M., Kaplan, I.R., 1983. Isotopic inferences of ancient biochemistries: carbon, sulfur, hydrogen, and nitrogen. In: Schopf, J.W. (Ed.), Earth's Earliest Biosphere: Its Origin and Evolution. Princeton University Press, Princeton, NJ, pp. 149–186.

Semikhatov, M.A., 1991. General Problems of Proterozoic Stratigraphy in the USSR. Harwood Academic Publishers. London, 192 pp.

Sergeev, V.N., Knoll, A.H., Kolosova, S.P., Kolosov, P.N., 1994. Microfossils in cherts from the Mesoproterozoic (Middle Riphean) Debengda Formation, the Olenek Uplift, northeastern Siberia. Strat. Geol. Correl. 2, 19–33.

Sogin, M.L., 1991. Early evolution and the origin of eukaryotes. Curr. Opinion Gen. Develop. 1, 457–463.

Sogin, M.L., 1994. The origin of eukaryotes and evolution into major kingdoms. In: Bengtson, S. (Ed.), Early Life on Earth. Columbia University Press, New York, pp. 181–192.

Sumner, D.Y., Grotzinger, J.P., 1996. Were kinetics of Archean calcium carbonate precipitation related to oxygen concentration? Geology 24 (2), 119–122.

Sun, D., Li, H., Lin, Y., Zhou, H., Zhao, F., Tang, M., 1991. Precambrian Geochronology, chronotectonic framework and model of chronocrustal structure of the Zhongtiao Mountains. Acta Geol. Sinica 65 (4), 216–231.

Sun, S., Cong, B., Li, J., 1981. Evolution of Henan–Shaanxi sedimentary basin of the Middle and Late Proterozoic age (I). Scientia Geol. Sinica 4, 314–322.

Sun, S., Chen, Z., Wang, Q., 1982. Evolution of Henan–Shaanxi sedimentary basin of the Middle and Late Proterozoic age (II). Scientia Geol. Sinica 1, 5–12.

Sun, W., Wang, G., Zhou, B., 1986. Macroscopic worm-like body fossils from the Upper Precambrian (900–700 Ma), Huainan district, Anhui, China and their stratigraphic and evolutionary significance. Precambrian Res. 31, 377–403.

Thrailkill, J., 1976. Speleothems. In: Walter, M.R. (Ed.), Developments in Sedimentology 20: Stromatolites. Elsevier, Amsterdam, pp. 73–86.

Tianjin Institute of Geology and Mineral Resources, Nanjing Institute of Geology and Palaeontology, Geological Survey of Inner Mongolia, 1979. Study of the Sinian Subera Stromatolites from Jixian, North China. Geological Publishing House, Beijing, 94 pp (in Chinese).

Vidal, G., Dawes, P.R., 1980. Acritarchs from the Proterozoic Thule Group, North-West Greenland. Grønl. Geol. Unders. Rep. 100, 24–29.

Wang, H., (Ed.), 1985. Atlas of the Palaeogeography of China. Cartographic Publishing House, Beijing, 143 pp.

Xing, Y., 1989. The Upper Precambrian of China. The Stratigraphy of China, vol. 3. Geological Publishing House, Beijing, 314 pp (in Chinese with English abstract).

Yan, Y., Zhu, S., 1992. Discovery of acanthomorphic acritarchs from the Baicaoping Formation in Yongji, Shanxi and its geological significance. Acta Palaeontol. Sinica 9 (3), 267–282.

Yin, L., 1985. Microfossils of the Doushantuo Formation in the Yangtze Gorge District, western Hubei. Palaeontol. Cathayana 2, 229–250.

Yin, L., 1987. Microbiotas of latest Precambrian sequences in

China. In: Nanjing Institute of Geology and Palaeontology, Academia Sinica (Ed.), Stratigraphy and Palaeontology of Systemic Boundaries in China, vol. 1, Precambrian–Cambrian Boundary. Nanjing University Press, Nanjing. pp. 415–494.

Yin, L., 1997. Acanthomorphic acritarchs from Middle–Upper Proterozoic shales of the Ruyang Group in Shanxi, China. Rev. Palaeobot. Palynol., to be published.

Yin, L., Li, Z., 1978. Precambrian microfloras of southwest China, with reference to their stratigraphic significance. Mem. Nanjing Inst. Geol. Palaeont. Acad Sinica 10, 41–108.

Zhang, W., Zhu, Z., 1979. Notes on some trilobites from Lower Cambrian Houjiashan Formation in southern and southwestern parts of North China. Acta Palaeontol. Sinica 18 (6), 513–526.

Zhong, F., 1977. On the Sinian geochronological scale of China based on radiometric dates on the Sinian strata in the Yanshan area. Scientia Sinica 2, 151–161.

Zhong, H., Chen, J., 1992. Carbon isotopic evidence for low bioproductivity 1.4 Ga ago. Scientia Geol. Sinica 2, 160–168.

Zhou, X., Zhang, Z., 1991. Microflora and sedimentary environment of the Wumishan Formation (Jixian System), Ming Tombs region, Beijing. Acta Micropalaeontol. Sinica 8, 289–300.

Zhu, S., Yan, Y., Chen H., 1994. The Middle-Upper Proterozoic on southern margin of North China Platform. In: Zhu, S., Xing, Y., Zhang, P. (Eds.), Biostratigraphic Sequence of the Middle–Upper Proterozoic on North China Platform. Geological Publishing House, Beijing, pp. 192–200 (in Chinese with English abstract).